Laser and Particle Beams (1996), *vol.* 14, *no.* 3, *pp.* 393–438
Printed in the United States of America

Physical mechanisms leading to high currents of highly charged ions in laser-driven ion sources

By HELMUT HASEROTH* AND HEINRICH HORA**
*CERN PS, 1211 Geneva, Switzerland
**University of New South Wales, Sydney 2052, Australia, and Anwenderzentrum, Institute of Technology, Hermann-Geib-Str. 18, 93053 Regensburg, Germany

(Received 12 April 1996; accepted 17 April 1996)

Heavy ion sources for the big accelerators, for example, the LHC, require considerably more ions per pulse during a short time than the best developed classical ion source, the electron cyclotron resonance (ECR) provides; thus an alternative ion source is needed. This can be expected from laser-produced plasmas, where dramatically new types of ion generation have been observed. Experiments with rather modest lasers have confirmed operation with one million pulses of 1 Hz, and 10^{11} C^{4+} ions per pulse reached 2 GeV/u in the Dubna synchrotron. We review here the complexities of laser–plasma interactions to underline the unique and extraordinary possibilities that the laser ion source offers. The complexities are elaborated with respect to keV and MeV ion generation, nonlinear (ponderomotive) forces, self-focusing, resonances and "hot" electrons, parametric instabilities, double-layer effects, and the few ps stochastic pulsation (stuttering). Recent experiments with the laser ion source have been analyzed to distinguish between the ps and ns interaction, and it was discovered that one mechanism of highly charged ion generation is the electron impact ionization (EII) mechanism, similar to the ECR, but with so much higher plasma densities that the required very large number of ions per pulse are produced.

1. Introduction

Since the first studies of laser interaction with solid targets in vacuum, the study of the generated ions (Lichtman *et al.* 1963; Ready 1971) and electrons (Ready 1965) was of special interest, and the first most shocking anomalies of the laser–plasma interaction were observed just from these observations of particle emission. Despite the heftiest protests by Ready (1965) observing fully classical electron emission with emission currents following the space charge limitations of the Langmuir–Child law, it was Honig (1963) who first published that these currents could be more than 1000 times higher than these space charge limitations. And while Ready (1971) observed ion energies of a few eV according to the classical interaction process with plasmas of some 100,000 Kelvin temperature, Linlor observed ion energies more than 1000 times higher as soon as the laser power exceeded the magic threshold of about 1 MW.

Apart from the fascination and challenge about these most unexpected phenomena, the ideas to use this emission of electrons or of ions as sources for accelerators and other purposes were evident, and a patent first was granted to Peacock and Pease (1969). The use of the mentioned energetic ions was of special interest for ion sources (Hora *et al.* 1980), especially for ion implanters for metal ions (Höpfl *et al.* 1995; Boody *et al.* 1996), for example, for reducing the friction of steel while increasing the strength.

The urgency for needing the laser ion source came rather late although highly meritorious work by Russian centers in Moscow (Phys.-Tech. Inst., ITEP), and Dubna was pub-

© 1996 Cambridge University Press 0263-0346/96 $11.00 + .10

Downloaded from https://www.cambridge.org/core. University of Basel Library, on 11 Jul 2017 at 11:30:36, subject to the Cambridge Core terms of use, available at https://www.cambridge.org/core/terms. https://doi.org/10.1017/S0263034600010119

lished before; see, for example, Haseroth *et al.* (1993). It became clear that the otherwise highly developed electron cyclotron resonance (ECR) source is limited by basic physical laws and can not immediately supply the ion numbers per pulse that are needed for the now-developed large hadron collider (LHC) at CERN for heavy ions. The most advanced ECR ion source produces 1.8×10^{10} of 27-time ionized lead ions per pulse of about ms duration (Hill *et al.* 1994). What has been achieved from a laser ion source even with rather modest laser pulses (Collier *et al.* 1996) are 1.5 mA Ta^{20+} ions with such small emittance fitting a radio frequency quadrupole (RPQ) providing an ion source of 100 keV/nucleon (Kugler, Haseroth *et al.* 1996). The pulse duration of 5 μs after the RFQ just fits the requirements of the LHC. What is needed for the LHC is 10 mA in 5μs.

This paper summarizes the physics problems of the generation of the ions from a target when laser light is irradiated. The questions of the guiding of these ions for injecting them into the beam optics of an accelerator, for example, a linac, are not discussed in this paper.

The reason why we try to describe comprehensively the numerous phenomena that can happen at laser interactions with targets and with the generated plasmas, and to discuss these results in view of the present knowledge of physics, is mainly to illustrate the complexity of the phenomena. This is to teach each newcomer to the field, who simply may assume that laser–plasma interactions can be described by primitive hydrodynamic differential equations, how the interaction with laser powers less than MW (Ready 1971) for material treatment with lasers may work. The mechanisms at higher laser powers up to relativistic intensities are much more complex, as the initially mentioned examples of Honig (1963) and Linlor (1963) demonstrated in the very early days of this field, or as the generation of 52-time ionized gold ions with energies of 0.4 GeV demonstrated (Begay *et al.* 1985) or the 6 GeV ions (Gitomer 1984). Recent experiments produced T_a^{53+} ions with 4.8 MeV energy using 50 J–350 ps iodine laser pulses (Woryna *et al.* 1995).

What can be said about these phenomena and what is proven knowledge are the aims of this paper. An additional aspect is that the appropriate application of ion sources with the mentioned special properties will provide many more new properties for laser ion sources than are common now from experiments with medium laser powers.

One essential aspect is that the use of medium-level laser pulses without the special advantages of using nonlinear effects and other advancements of the physics of laser–plasma interaction for laser ion sources can provide special conditions of electron impact ionization (EII) (Hora *et al.* 1992) that are similar to the classical ion electron cyclotron resonance (IEC) source. However, the very much higher electron density in the laser-produced plasmas (although only of short duration) provides the much larger ion number per pulse than in the classical IEC.

2. Review of relevant results for the laser ion source

Although we have mentioned some of the very diverging observations of laser interaction with targets and plasma in the introduction, we shall elaborate on these initial facts further in view of the mentioned pioneering experiments of the laser ion sources of the preceding years, of the Moscow and Dubna groups, with remarkable achievement of ion pulses in high-energy accelerators.

2.1. *General overview*

We first present in this subsection an overview of observed phenomena of ion production by lasers for an ion source. A typical measurement of ion energies from the time of flight is shown in figure 1a. A CO_2 laser of varying intensity $I = \Phi$ in W/cm^2 is shown, where at the lowest intensity of 10^{12} W/cm^2 a first narrow peak can be recognized which

Downloaded from https://www.cambridge.org/core. University of Basel Library, on 11 Jul 2017 at 11:30:36, subject to the Cambridge Core terms of use, available at https://www.cambridge.org/core/terms. https://doi.org/10.1017/S0263034600010119

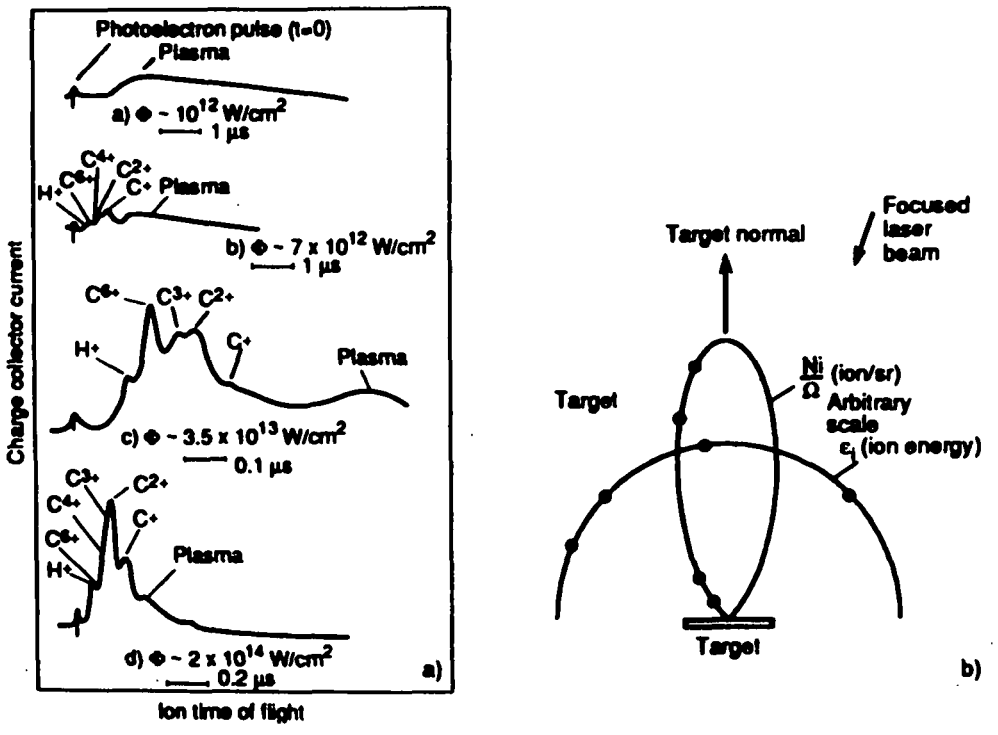

FIGURE 1. Ion emission of up to 2-MeV energy from carbon-dioxide laser-irradiated carbon and aluminum (Ehler 1975). (a) Oscilloscope signals for various laser intensities. (b) Angular distribution.

corresponds to the photoemission of electrons from the probe due to the UV photons of the laser-produced plasma. This is an ideal mark for the time zero (neglecting the speed of light for the photons between the target and the probe). The signal that follows later corresponds to the ions of the more or less thermalized, expanding plasma. At higher intensities there are maxima appearing in the ion signal corresponding to very high ion energies that are much above the thermal properties. Energetic ions of this type have been observed since the first multikiloelectronvolt ions were detected by Linlor (1963) with ruby laser powers of only several megawatts, and always at these higher laser powers, in numerous experiments around the world.

The use of differentiating diagnostics with Thomson parabolas and other electrostatic or magnetostatic analysers confirmed that there were truly highly charged ions observed, for example (Ehler 1975), Al^{13+}, or much higher ionization states from other elements, for example (Bykovskii *et al.* 1971; Apollonov *et al.* 1990), Co^{27+}. The energetic ions could contain 80% of the whole ion energy (Ehler 1975) and show a strong directivity perpendicular to the target (figure 1b). In this case, 2.7×10^{14} ions were counted as being energetic ions whose energy was 200 keV for singly charged aluminum linearly increasing in dependence on the charge number to $Z = 11$, where the ion energy was about 2 MeV. Apart from the very fast megaelectronvolt ions and the low energetic thermal ions, there was a third group of plasma detected between the two groups (Ehler 1975). The additional diagnostics permitted a differentiation of the aluminum ions of the higher charge numbers of the target from precursing hydrogen ions or carbon and hydrocarbon ions owing to contamination by the oil from the vacuum pumps. The explicit clarification of megaelectron-

Downloaded from https://www.cambridge.org/core. University of Basel Library, on 11 Jul 2017 at 11:30:36, subject to the Cambridge Core terms of use, available at https://www.cambridge.org/core/terms. https://doi.org/10.1017/S0263034600010119

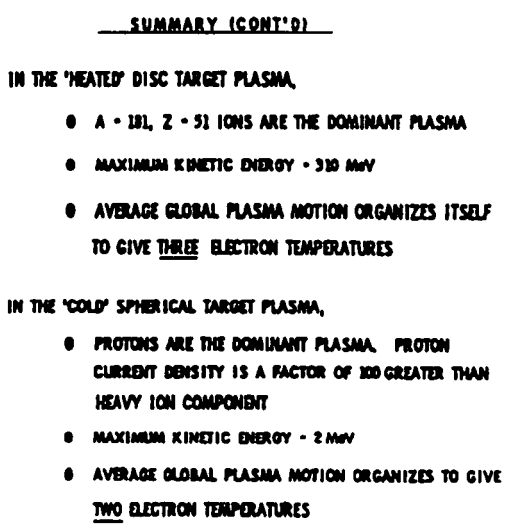

FIGURE 2. Reproduction of the reported measurement of laser-produced 310-MeV Au^{51+} ions (Begay *et al.* 1983).

volt ions was reported from tungsten targets (Siegrist *et al.* 1976). The fact that these ions not only could be diagnosed by time-of-flight measurement, but really got their high mega-electronvolt energy from the spot of their origin within the target at the area of laser interaction, could be confirmed by Rode (1983) and Basov *et al.* (1987), who measured the X-ray spectra of phosphorous ions in the range of a few angstrom and saw, for example, the Doppler shift of p^{13+} ions of 2 MeV by irradiation intensities of 2×10^{15} W/cm^2 of a neodymium glass laser.

Using the Helios CO_2 laser, Au^{51+} with maximum ion energies of 310 MeV were measured [see figure 2, which is a copy of an overhead projection (Begay *et al.* 1983; Gitomer *et al.* 1986), since this fact was not published elsewhere], while experimental results were related to ion energies per nucleon (see Section 4, especially figure 14) from which energies of gold ions of up to 500 MeV can be confirmed (Gitomer *et al.* 1986). For an extension of the measurements from the Helios to the very large ANTARES laser, a very sophisticated numerical evaluation (Jones *et al.* 1982) resulted in the prediction of ion energies up to 5 GeV in agreement with later measurements (Gitomer, 1984).

These facts alone were most impressive when considering the laser ion source as a candidate for use in accelerators. Numerous other problems, however, had and still have to be clarified beforehand. There is the question of the thermal width of the highly charged energetic ions and how this can be solved by accelerator techniques; there is also the problem of the extraction of the ions after their generation for the subsequent preacceleration by injection into a linac, or quadrupole accelerator, or a cyclotron, and many more questions (Amdidouche *et al.* 1992).

2.2. *Developments of an ion source for injection by a linac*

One further point of importance is the technology of the lasers and the engineering of the target for a very large number of high repetition rates and fully reliable functioning of the laser ion source. These developments have succeeded, for example, at 1-Hz opera-

Downloaded from https://www.cambridge.org/core. University of Basel Library, on 11 Jul 2017 at 11:30:36, subject to the Cambridge Core terms of use, available at https://www.cambridge.org/core/terms. https://doi.org/10.1017/S0263034600010119

tion for more than one million pulses (Sharkov *et al.* 1992) or for filling 4000 shots of 1 Hz of magnesium ions into an accelerator, in each finally producing pulses of 10^9 C^{5+} or of 10^8 Mg^{12+} or of 9×10^{10} C^{4+} in a proton synchrotron with energies of 2 GeV/u after injection through a linac (Mochinski 1991). We shall report on these technological developments in the following paragraphs of this subsection, while the physics is discussed in detail in the following sections.

Research and development on the laser ion source have been pioneered since about 1969 by Prof. Yu. A. Bykhovski of the Engineering Physics Institute in Moscow, whose work also has been followed up by his co-workers in other institutes, such as the JINR, Dubna, or the ITEF in Moscow. The problems involved are still rather complex, since a number of anomalous processes known from laser fusion research are involved; these refer to the properties of the recombination of ions, including the appearance of negative ions, while the main studies are the usual detection of highly ionized heavy ions, their angular distribution and interaction with magnetic fields, their bending and selection by fields, and their injection into accelerators. For applications in mass spectroscopy, see Phipps *et al.* (1993) and Phipps (1995).

While the thermal and rather anomalous nonlinear properties of the ions from laser-produced plasmas were studied intensively in scientific laboratories around the world, the application for ion sources in accelerators first was discussed in the Western countries by Peacock and Pease (1969) at the Culham Laboratory before 1968 and in patents. Later work (Omari *et al.* 1980; Hughes *et al.* 1980; Korschinek *et al.* 1986) was strongly supported by the results achieved after many years by the above-mentioned Moscow Institute.

Some unique results of the Munich ion source (Korschinek *et al.* 1986) will be discussed, especially in Section 8. The work with the classical proton synchrotron at Dubna, mostly favored by N. G. Flerov, is the longest known activity for filling accelerators with laser-produced plasmas. Monchinski (1991) now uses transversely excited atmospheric pressure (TEA) carbon-dioxide lasers. He used neodymium glass lasers in the 1970s, but did not find them very useful—at least at the low energies and high repetition rates that were available up until about 1980. Monchinski's carbon-dioxide laser has a typical 100-ns first pulse and a subsequent long pulse of about equal energy of 1- to 2-μs length. The laser has been modified in such a way that the long pulse can be switched off within the laser cavity (obviously a rather new modification). The target chamber that can be used with most uncomfortable solid targets, including magnesium, contains a cylindrical target that can be rotated step by step for each shot. Liquid metal at the same spot as the target is under experimentation. With the present cylindrical rotating target, 4000 shots of 1-Hz sequence in each run have been performed without opening the chamber. The salt entrance lens of the laser beam was protected against the emitted ions by a plastic foil that was designed so that it could be removed from the front of the lens and renewed automatically after a number of shots.

The ion beam is injected through a tube about 3 m in length to an ion-bending system, turning the beam about 35° and selecting the ions of desired ionization into the axis of a following linac. After this the ions are guided into Dubna's first proton synchrotron. The linac is for 20 MeV protons and 5 MeV/u ions. An e/m ratio of 1/3 is the limit before breakdown occurs.

The carbon-dioxide laser produces a first pulse of 7 J total energy, with 30 MW and 100 ns duration. The following long pulse tail is cut off. This was considered necessary for high fluxes for higher charged ions; otherwise, the long pulse could be used. For the synchrotron, 20-μs long pulses of C^{4+} have been produced, resulting in 5×10^{10} C^{4+} ions with an energy of 4 GeV/u in the synchrotron. Up to 10^9 C^{5+} and 10^8 Mg^{12+} ions were produced without the laser pulse tail and consisted of 5-μs pulses.

Downloaded from https://www.cambridge.org/core. University of Basel Library, on 11 Jul 2017 at 11:30:36, subject to the Cambridge Core terms of use, available at https://www.cambridge.org/core/terms. https://doi.org/10.1017/S0263034600010119

2.3. *Laser ion source using cyclotrons*

An alternative method of generating ions from a laser-produced plasma for injection into a linac is to generate the ions at the central axis of a cyclotron. This is being studied, especially for the source of heavy ions, in a project at Dubna under the direction of Yu. Z. Oganesian. The existing 2-m or 4-m cyclotrons are used as described below. Moderate- and high-repetition-rate laser pulses have produced up to 10^{10} ions of C^{3+} or ten times less Si^{7+} ions in the synchrotrons into which the ions were injected after leaving the cyclotron. This was reported by Kutner *et al.* (1990), who referred to earlier work (Barabash *et al.* 1984).

A 10-J carbon-dioxide laser pulse of 60 ns duration produces 18 times more ionized niobium with a laser intensity of 3×10^{10} W/cm^2. The ions are produced in a tube (figure 3) in the central axis of a cyclotron of 2 or 4 m diameter with a laser irradiation from above. The cyclotron magnetic field B also acts inside the tube so that the plasma generated from the target (figure 3) expands as a slim plume within the tube. When passing the grids of high voltages, ions of desired specifications are extracted into the cyclotron and subsequently accelerated. After the cyclotron, the ions are injected into a linac, reaching an energy of 10 MeV/u before going to the synchrotron. Including a mechanism with an "exotic beam" for charge exchange, they achieved the above-mentioned pulses of C^{3+} ions of 10^{10} and ten times less ions in Si^{7+} pulses. However, the pulses after the 2-m cyclotron are very long, of 5-μs duration. Ten times shorter pulses are needed to better fit the circumference of the following synchrotron.

The configuration is ideal for the cyclotron since its magnetic field is simultaneously used for the guiding of the plasma plume. The scheme has been studied with small laser pulses of 1.5 J energy only, and with 10^{10} W/cm^2 intensity, where Fe^{+12} ions have been produced.

It was also possible to work with neodymium glass laser pulses as low as 50 mJ and 2×10^9 W/cm^2 intensity to achieve C^{+3} with 1.5×10^{10} ions per pulse. Since there was an instability of the plasma observed in the magnetic field parallel to the plume, a metallic cylinder was introduced around the plasma plume that fully stabilized the plasma.

Further tests were performed to see what would happen if the magnetic field was not parallel to the plasma plume, as in figure 3, but perpendicular to it. In this case, the target was in front of the electrostatic grid for the extraction of the ions into the cyclotron. The

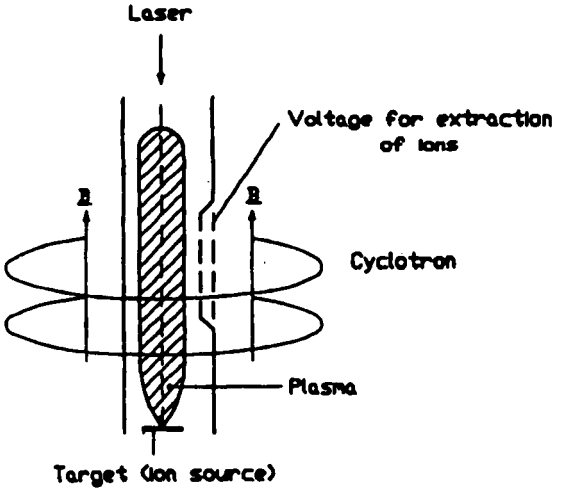

FIGURE 3. Laser ion source in the axis of a cyclotron with an extraction voltage (Kutner *et al.* 1990).

Downloaded from https://www.cambridge.org/core. University of Basel Library, on 11 Jul 2017 at 11:30:36, subject to the Cambridge Core terms of use, available at https://www.cambridge.org/core/terms. https://doi.org/10.1017/S0263034600010119

laser had to be obliquely incident at 45°. Carbon-dioxide laser pulses of 10 J, 60-ns duration, and 3×10^{10} W/cm^2 intensity were used. Once again, Nb^{18+} was observed, but the ion distribution showed a butterfly-wing profile. This was due to the charge separation by the magnetic field, and a further action of the magnetohydrodynamically generated electric field was expected. The details of the mechanisms are not yet understood. It was suggested that the $\mathbf{E} \times \mathbf{B}$ drift of plasma has to be included to describe the plasma motion. The result is that 1000 times more ions for 14 times ionized Ta have been observed.

Most of these experiments concerning technological developments of laser ion sources used only medium-size or even smaller lasers, where the main properties of the ions in the usual cases were of a thermal nature; they did not have the supra thermal properties of the above-mentioned energetic ions. We shall come back to this question after reporting on the known general physical problems of laser interaction with plasma.

3. Physics of laser ion sources

As was mentioned in the preceding section, the laser interaction with solid targets in vacuum generates plasma with a complex property of the emitted ions. These phenomena can be advantageous or may cause difficulties for the laser ion sources. For this reason we present here a short review of the physics of the phenomena involved. This was summarized in several reviews (Eliezer *et al.* 1989; Meyers 1986; Bobin 1985; Key 1991) and monographs (Ahlstrom 1983; Hora 1991; Velarde *et al.* 1993), where the main interest of the applications was not so much the laser ion source but the use of the lasers for igniting exothermal thermonuclear fusion reactions.

This broad field of research indicated in much detail how the complexity and difficulty of the interaction mechanism are due to nonlinearities of the hydromechanical properties of the generated plasma (nonlinear forces) and the nonlinearity of the optical constants when these depend on the laser intensity. These forces not only will lead to the unique cavitons, but also to the linear separation of the very fast ions, depending on their charge. The involved mechanism of self-focusing is described in the following section. One phenomenon observed was the generation of suprathermal "hot" electrons and resonances (Section 5), while the mechanism of parametric instabilities was a topic of very intensive studies (Section 6).

In order to analyze the nonlinear forces of laser–plasma interactions, the properties of the highly inhomogeneous plasmas, which caused the internal electric fields and double layers in plasmas, had to be studied. The earlier known ambipolar fields were a special case, only of a much more general oscillating phenomenon with consequences of surface tension contrary to any earlier expectations (Section 7). The most complex property of laser–plasma interaction was understood within the last few years only by the experimental confirmation of a very irregular temporal pulsation, or stuttering, in the range of 10 to 40 ps duration (Section 8). Some intuitively introduced optical methods for the smoothing of the interaction appeared to be very successful in overcoming this pulsation problem, although the reason for which these smoothing methods were introduced was motivated by the need to solve a different problem.

Only now, after 30 years of laser–plasma interaction studies covering the most advanced diagnostics and experimental techniques with resolutions in the range down to picoseconds or less and micrometers (Ahlstrom 1983; Basov *et al.* 1986), a solution may have been found for the physical understanding of direct drive (Hora 1991; Velarde *et al.* 1993) laser interactions with plasmas for fusion. We also know now what physics phenomena will be covered for the development of the laser ion source. In fact, the study of the laser ion source (Korschinek *et al.* 1986) produced, in a very independent and unintentional way, results

Downloaded from https://www.cambridge.org/core. University of Basel Library, on 11 Jul 2017 at 11:30:36, subject to the Cambridge Core terms of use, available at https://www.cambridge.org/core/terms. https://doi.org/10.1017/S0263034600010119

that confirm the very recent view of the physics solution of the laser–plasma interaction, as will be discussed in Section 8.

We discuss now the nonlinearities in hydromechanics and optical response. As was mentioned concerning the phenomena of the laser ion source, the surprising and confusing results of laser interaction with plasmas appeared simply from the study of the ion energies from laser-produced plasmas. When the laser power was less than about 1 MW, the generated plasma behaved absolutely classically, with temperatures of a few thousand degrees (a few electronvolts). The electron emission was also fully classical (Ready 1965), with emission current densities of about 100 mA/cm^2, exactly as limited by the Langmuir–Child space-charge law. However, when applying laser pulses of more than 1 MW power, a basic change appeared (Honig 1963): The electron current densities—contrary to what was expected from the mentioned space-charge limitations—arrived at 10 to 100 A/cm^2.

The ions that had maximum energies suddenly changed from a few electronvolts for laser powers below megawatt to kiloelectronvolt above megawatt (Linlor 1963) had a clearly superlinear, nearly quadratic increase on the laser power (Hora 1991, fig. 1.1; Isenor 1964; Schwarz 1971) which, however, for higher laser powers arrived at some saturation with an exponent of less than one at higher powers (figure 4) (Hora 1991). These nonlinear fast ions flying preferentially against the laser light with energies of several kiloelectronvolts could be seen directly from image converter pictures (Engelhardt *et al.* 1970; Hora 1971); see figure 5. On ruby laser irradiation with 2 to 10 J pulses of 10 to 20 ns duration on spherical aluminum of a few 100 μm diameter in the laser focus, a central spherical plasma was produced which fully followed a gas dynamical expansion with temperature between 10 and 70 eV (Hora 1971), exactly as predicted numerically from the Zeldovich–Reiser model as used by Basov and Krokhin (1963) and Dawson (1964), and which was improved by taking into account the temporal increase of the radius during the interaction (Hora 1991, fig. 5.1).

The outer part of the plasma with maximum ion energies up to 10 keV moving asymmetrically toward the laser showed a typically nonlinear behavior where the maximum ion energies increased with an exponent of nearly 1.5 over the laser intensity. Under the conditions of this experiment, the amount of energy being transferred to the nonlinear part of the plasma was about 5%, while the thermal plasma consumed nearly 95% of the inter-

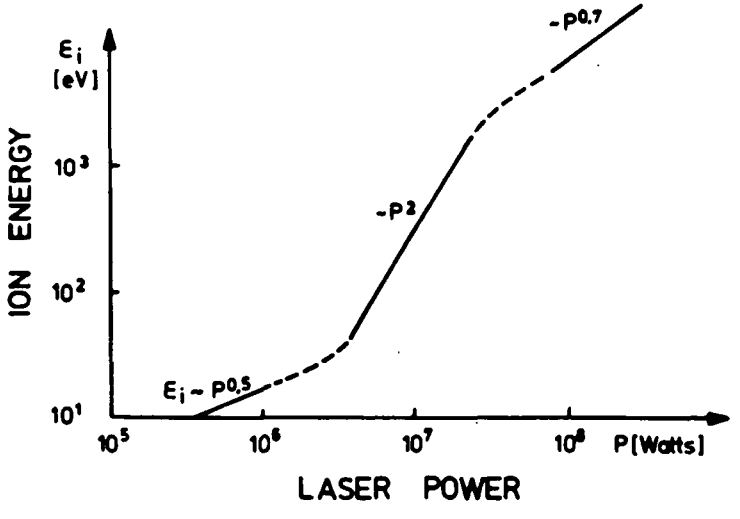

FIGURE 4. Maximum ion energy of thermal properties below about 1-MW laser irradiation and superlinear increase to keV ions above MeV with some saturation at higher laser powers (Hora 1991).

Downloaded from https://www.cambridge.org/core. University of Basel Library, on 11 Jul 2017 at 11:30:36, subject to the Cambridge Core terms of use, available at https://www.cambridge.org/core/terms. https://doi.org/10.1017/S0263034600010119

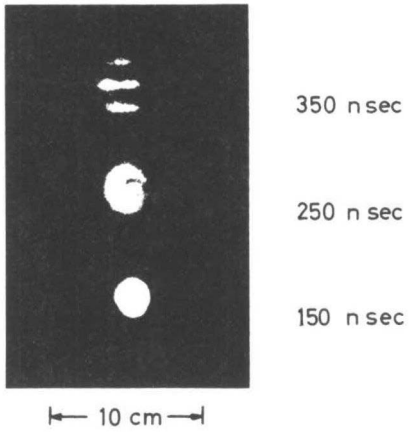

FIGURE 5. Side-on framing camera pictures of laser-irradiated aluminum spheres (from the left-hand side) showing the central thermal plasma of some 10-eV temperature and the asymmetric (half-moon-like) keV ions moving with preference against the laser light (Engelhardt *et al.* 1970; Hora 1971).

acting laser energy. This should be mentioned in view of the experimental result that under conditions of much higher laser intensities, the equivalent intensity of CO_2 lasers comparable with that of ruby lasers is to be converted by factor of 100 because of the $I\lambda^2$ law (Hora 1991) for intensity I and wavelength λ as shown in figure 4, and 90% of the interacting laser energy went into the fast ions of more than 100 keV energy (Ehler 1975).

There was an initial discussion as to whether the kiloelectronvolt ions generated in the plasmas, whose temperatures were only some electronvolts, are produced in the electric field of the plasma surface. The light electrons at this temperature leave the plasma with high velocities, leaving behind the heavy ions and generating an electric field corresponding to a double layer (see Section 7). If an ion is speeded up by this ambipolar electric field to the electron velocity, kiloelectronvolt energies are produced immediately. The problem is, however, that this double layer has the thickness of a Debye length; therefore, only about 10^9 or less ions can be accelerated in this way. This has been shown experimentally for a group of fast ions from a laser-produced plasma of about the same number where no dependence on the polarization of the light has been detected (Wägli *et al.* 1979).

Since the number of ions of kiloelectronvolt energy was 10^{14} and more from the beginning (Linlor 1963) and was reproduced continuously in all other known experiments (Hora 1991), the electrostatic mechanism for the acceleration could not be applied, at least not for the main part of the kiloelectronvolt ions. This was the motivation to look for nonlinear hydrodynamical processes of the laser interaction with plasma. The first result was that forces of direct electrodynamic interaction without heating the plasma dominate any gas-dynamic force density (the negative gradient of the gas-dynamic pressure P) if the laser intensity is sufficiently high, that is, higher than 10^{14} W/cm^2 for neodymium glass lasers and 100 times less for carbon-dioxide layers [with respect to the $I\lambda$ law (Hora 1991)]. The essential reason for the force was that the gradient of the plasma density as expressed by the complex refractive index $\tilde{n}$ was determining the force called a "nonlinear force," (see the difference to the ponderomotive potential, Hora, 1996). For perpendicular incidence of the laser wave on a striated plasma, the force was (Hora *et al.* 1967; Hora 1969, 1985, 1991)

$$\mathbf{f}_{NL} = -(1 - |\tilde{n}|^2)\,\frac{\mathbf{E}^2}{16\pi}\,\frac{\partial}{\partial x}\,\frac{1}{|\tilde{n}|}. \tag{1}$$

Downloaded from https://www.cambridge.org/core. University of Basel Library, on 11 Jul 2017 at 11:30:36, subject to the Cambridge Core terms of use, available at https://www.cambridge.org/core/terms. https://doi.org/10.1017/S0263034600010119

The refractive index $\tilde{n}$ is given by

$$\tilde{n}^2 = 1 - \frac{\omega_p^2}{\omega^2(1 - i\nu/\omega)}, \tag{2}$$

where ω is the laser radian frequency, ω_p is the plasma frequency given by

$$\omega_p^2 = \frac{4\pi e^2}{m_e} n_e, \tag{3}$$

e being the charge, m the mass, and n_e the density of the electrons in the plasma, and

$$\nu = 8.51 \cdot 10^{-1} \frac{Zn_e}{T^{3/2}} \ln[1.55 \cdot 10^{10} T^{1/2}/(Zn_e^{1/2})] \tag{4}$$

being the collision frequency (Hora 1991) of the electrons with ions in the plasma having a temperature T. The time-averaged nonlinear force density in the case of general geometry for nearly stationary (nontransient) incident laser pulses was shown to be (Hora 1989)

$$\mathbf{f}_{NL} = \frac{1}{c} \mathbf{j} \times \mathbf{H} + \frac{1}{4\pi} \mathbf{E}\nabla \cdot \mathbf{E} + \frac{1}{4\pi} \nabla \cdot (\tilde{n}^2 - 1)\mathbf{E}\mathbf{E} \tag{5a}$$

$$\mathbf{f}_{NL} = \nabla \cdot \left[\mathbf{T} + \frac{\tilde{n}^2 - 1}{4\pi} \mathbf{E}\mathbf{E} \right] - \frac{1}{4\pi c} \frac{\partial}{\partial t} \mathbf{E} \times \mathbf{H}, \tag{5b}$$

where $\mathbf{E}$ and $\mathbf{H}$ are the electric and magnetic laser field strengths, $\mathbf{j}$ is the current density in the plasma, and $\mathbf{T}$ is the Maxwellian stress tensor. The correctness of the formulation, and of this formulation only, was proved by the conservation of momentum. Any adding or subtracting of nontrivial terms of equations (5a) and (5b) results in an imbalance of the momentum. The tensor algebraic equivalent of equation (5b) derived from equation (5a) is the first *hydrodynamic* derivation of the Maxwellian stress tensor (instead of the historic *elastomechanic* derivation), and it occurred for the first time at the force density in the dispersive and dissipative case for plasma of any frequency while an earlier derivation of equation (5b) was for nondispersive, nondissipative dielectric fluids for moderate frequencies only, as was shown by Landau and Lifshitz (see Hora 1969, 1991).

Equation (1) is the special geometric case resulting from equations (5a) and (5b), and is formally identical with the ponderomotive force known since 1846 as electrostriction in electrostatics. It is also identical in high-frequency fields with gradients in the average intensity, for example in standing waves or in stationary beams (see Weibel and Kibble in Hora 1991). However, the result (1) showed for the first time the effect of the explosive effect of the dielectric inhomogeneity of the laser-irradiated plasma. The suggestion that the laser light causes a dielectric explosion was splendidly confirmed numerically by Shearer *et al.* (1970) (figure 6). While any gas-dynamic interaction will result in monotonous density profiles of the plasma, the nonlinear force produced a density minimum (caviton) as a result of the dielectric explosion. This caviton has been measured by numerous authors (Hora 1991) since 1975 as proof of the predominance of the nonlinear force over the thermokinetic forces.

For the case of fast time-dependent laser irradiation, a serious controversy appeared concerning the additional terms of equations (5a) and (5b), where six different schools have six different formulations (Zeidler *et al.* 1985). These formulations were still for approximative time dependences only and, by adding a further term, the closed formulation of the complete transient solution was derived (Hora 1985) as

Downloaded from https://www.cambridge.org/core. University of Basel Library, on 11 Jul 2017 at 11:30:36, subject to the Cambridge Core terms of use, available at https://www.cambridge.org/core/terms. https://doi.org/10.1017/S0263034600010119

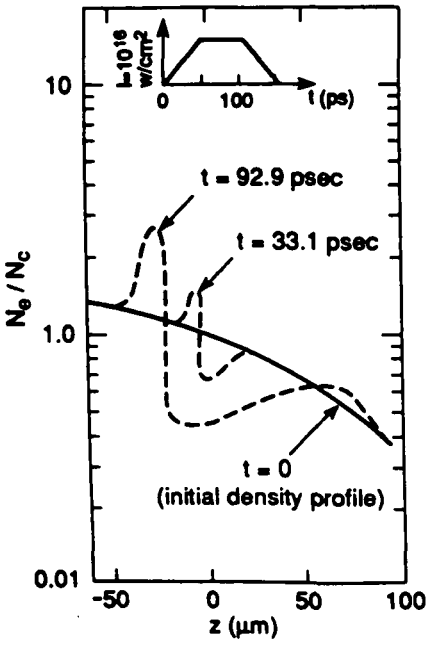

FIGURE 6. Computations of a plasma density profile with an electron density N_e related to the critical density $N_c = 10^{21}$ cm^{-3} of neodymium glass lasers for a laser pulse as shown in the upper diagram incident from the right-hand side for various times t with the discovery of the density minima (cavitons) generated by the action of the nonlinear force; from Shearer *et al.* (1970).

$$\mathbf{f}_{NL} = \frac{1}{c}\mathbf{j}\times\mathbf{H} + \frac{1}{4\pi}\mathbf{E}\nabla\cdot\mathbf{E} + \frac{1}{4\pi}\left(1+\frac{1}{\omega}\frac{\partial}{\partial t}\right)\nabla\cdot\mathbf{EE}(\tilde{n}^2-1) \tag{6a}$$

$$f_{NL} = \nabla\cdot\left[\mathbf{EE}+\mathbf{HH}-\frac{1}{2}(\mathbf{E}^2+\mathbf{H}^2)+\left(1+\frac{1}{\omega}\frac{\partial}{\partial t}\right)[\tilde{n}^2-1]\mathbf{EE}\right]\Big/4\pi - \frac{1}{4\pi c}\frac{\partial}{\partial t}\mathbf{E}\times\mathbf{H}, \tag{6b}$$

the general validity of which was proved by Lorentz and gauge invariance (Rowlands 1990).

While the general gas-dynamic and nonlinear forces for a hydrodynamic model of laser–plasma interaction have been established in this way, another nonlinearity to be discussed is the intensity dependence of the optical constants (2). The first modification appeared when the oscillation energy ϵ_{OSC} of the electrons in the laser fields of an intensity I expressed here in relativistic form,

$$\epsilon_{OSC} = m_0c^2[(1+3A(I)I/I_{rel})^{1/2}-1], \tag{7}$$

using a correction factor $A(I)$ monotonously growing from 1 for $I \ll I_{rel}$ with increasing intensity to 1.06 and using the relativistic threshold intensity I_{rel} (with the electron rest mass m_0 and the vacuum velocity c of light):

$$I_{rel} = 3m_0^2\omega^2c^3/(8\pi e^2). \tag{8}$$

The numerical value of equation (8) is

$$I_{rel} = 3\cdot10^{18}/\lambda^2 \qquad \text{W/cm}^2, \tag{9}$$

Downloaded from https://www.cambridge.org/core. University of Basel Library, on 11 Jul 2017 at 11:30:36, subject to the Cambridge Core terms of use, available at https://www.cambridge.org/core/terms. https://doi.org/10.1017/S0263034600010119

expressing the laser wavelength λ in micrometers. The relativistic threshold is that intensity where the oscillation energy of the electron in the laser field is mc^2 using the rest mass m_0 of the electron.

For high laser intensities I, the electron mass in the optical constants (2) to (4) has to be relativistically corrected to

$$m = m_0/(I - 3A(I)I/I_{rel})^{1/2}, \tag{10}$$

and the electron energy is then not only given by a chaotic motion due to a temperature T in equation (4), but also by an effective temperature

$$T_{eff} = T + \epsilon_{osc}/2k \tag{11}$$

using the Boltzmann constant k.

For high intensities, the collision frequency (4) is then dependent on the intensity I with a power of $-3/2$ as initially derived quantum mechanically by S. Rand and later from plasma theory [Hora 1991, Eq. (6.59)]. The question of the change of this exponent to $-1/2$, because of the quantum modification of the Coulomb collisions (Hora 1991) as an expression of the inclusion or neglect of stimulated emission in the ordinary inverse bremsstrahlung mechanisms, has been pointed out (Hora 1982, 1991), but may be an effect of academic interest only in laser-produced plasma processes at very high intensities.

While the nonlinear force was splendidly reconfirmed by numerical studies and experimentally as mentioned, the effects of the nonlinear optical responses for very high laser intensities were included only in the advanced numerical treatments.

What is important for laser ion source physics is the general dynamics by the nonlinear force with caviton generation and generation of ablation (and compression) velocities of the plasma block to such high values that never could be understood by thermal gasdynamics. One essential mechanism is the separation of the ions depending on their charges and the resulting linear increase of the ion energy on the charge number Z of the ions. There are no thermal (equilibrium) mechanisms that could explain this fact observed from a laser irradiated target.

This ion separation can be understood from one of the other derivations of the nonlinear force as it is known from the very beginning (Hora *et al.* 1967; Hora 1991) when the spatial dependence of the force on the gradient of the refractive index was discovered. Figure 7 shows the refractive index $\tilde{n}$ depending on the depths x of a 1D plasma irradiated perpendicularly by laser radiation. The quiver motion of the electron in the laser field in vacuum is an eight, which under stationary conditions is at rest at a certain depth x. Within the inhomogeneous plasma, the eight is swollen up due to the refractive index less than one. In a WKB-like (reflectionless) field, the oscillation energy of the quiver motion [see equation (7)] is given by its vacuum value $\epsilon_{osc,vac}$:

$$\epsilon_{osc} = \epsilon_{osc,vac}/|\tilde{n}|. \tag{12}$$

As is known from the first treatment (Hora *et al.* 1967), the net force is due to the phase shift between the **E** and the **H** vectors in the inhomogeneity. This leads to the fact that the swelled eight in the plasma (figure 7) is not at rest but drifting toward a lower plasma density. Finally, the electrons receive a translative (drift) energy ϵ_{trans}, which is the excess energy from swelling over the vacuum value:

$$\epsilon_{trans} = \epsilon_{osc}(1/|\tilde{n}| - 1) \approx \epsilon_{osc}/|\tilde{n}|. \tag{13}$$

For very high swelling (very low $\tilde{n}$) nearly the whole increased oscillation energy goes into translative motion. This energy goes into the ions whose mass to charge ratio m_i/Z

Downloaded from https://www.cambridge.org/core. University of Basel Library, on 11 Jul 2017 at 11:30:36, subject to the Cambridge Core terms of use, available at https://www.cambridge.org/core/terms. https://doi.org/10.1017/S0263034600010119

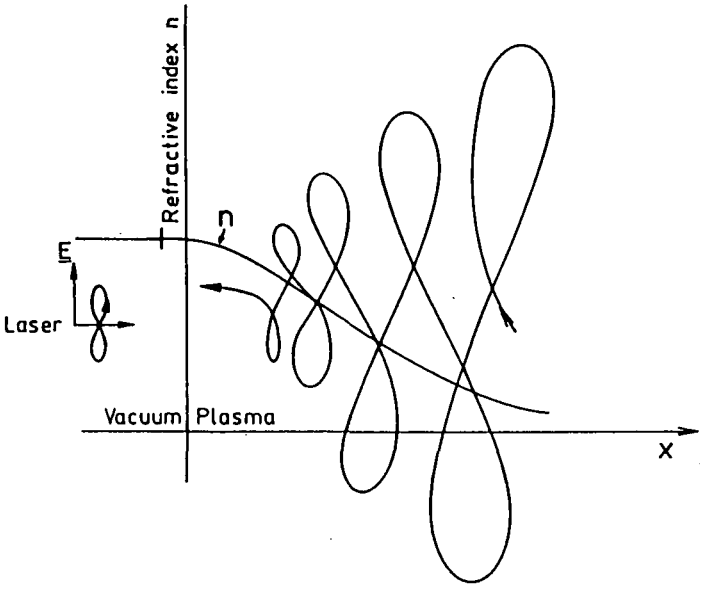

FIGURE 7. Refractive index n in an inhomogeneous plasma corona depending on the depth x with monotonously increasing electron density. If laser light is perpendicularly incident with the electric vector **E** polarized in the plane of the drawing, an electron performs a closed figure-eight-like motion in vacuum. Inside the plasma, the figure eight is swelled up [see equation (12)] due to the decreasing denominator $\tilde{n}$ to values 0.1 or much less] and the phase shift between **E** and **H** causes the electron to not stand in a figure eight but drift toward vacuum (toward the lower electron density).

determines the inertia when they are electrostatically attached to the electrons (apart from a small number of electrons needed to build up the necessary double layers). This leads to blocks of ions separated by their charges. The translative ion energies then are (Hora 1991) relating to the kinetic energy part of the oscillation energy,

$$\epsilon_i = Z\epsilon_{osc}/|\tilde{n}|, \tag{14}$$

showing how the observed linear Z-dependence of the fast (keV and more) ions are produced.

This generation of the fast ions, however, occurs easily at laser intensities $I\lambda^2$ (with the wavelength λ in micrometers) for values above 10^{14} W/cm^2 per micrometer square if, for example, plane wave conditions are to be considered. For lower laser powers, mechanisms of self-focusing (filamentation) (see the following section) appear which drive the laser intensities above the mentioned threshold and then can generate—by the nonlinear force acceleration processes—the keV ions. The threshold of the self-focusing—as will be shown—is just around MW laser power, which simply explains that the interaction with lower laser power results in a purely classical gas-dynamic expansion with energies in the eV or 10-eV range while above this threshold, and thus the surprising keV ions appeared.

4. Self-focusing (filamentation)

A crucial mechanism in laser-produced plasma is the self-focusing of the laser beams or of several parts of it in a plasma, producing filaments of rather small beam diameter. The

Downloaded from https://www.cambridge.org/core. University of Basel Library, on 11 Jul 2017 at 11:30:36, subject to the Cambridge Core terms of use, available at https://www.cambridge.org/core/terms. https://doi.org/10.1017/S0263034600010119

first self-focusing was observed when a laser beam of moderate power penetrated a dielectric medium. The second- and higher order intensity dependent terms of the dielectric constant caused a change in the initially plane-wave fronts of the beam, and normally was focused or periodically focused and defocused. The first theoretical model was published by Chiao *et al.* (1964) and resulted in a threshold of laser power (not intensity) from which point onward a laser beam is self-focused. The second-order dielectric coefficients were of the same value for the laser field as measured before by electrostatics. The thresholds for dielectrics were above 10^5 W for liquids such as CS_2 and 1000 times (approximately inversely proportional to the density) higher for air.

In plasmas there is no analogous nonlinear dielectric response. The basically different mechanisms of the nonlinear dynamics characterized by the ponderomotive force, however, result in self-focusing in plasmas.

In order to derive the threshold for self-focusing of a laser beam in a plasma, three physical mechanisms have to be combined. Assuming that the laser beam has a Gaussian intensity profile in the radial direction while propagating in the x-direction, the generated nonlinear force f_{NL} in the r-direction has to be compensated by the thermokinetic (Hora 1969a) force $\mathbf{f}_{th}$

$$\mathbf{f}_{th} = \mathbf{f}_{NL}, \qquad \nabla\cdot\left(\mathbf{T} - \frac{\tilde{n}^2 - 1}{4\pi}\,\mathbf{EE}\right) = \nabla n_e kT(1 + Z), \tag{15}$$

where use is made of equation (5b). The second physical mechanism is the total reflection of the laser-beam components starting under an angle α_0 from the center of the beam and bent into a direction parallel to the axis, owing to the density gradient of the plasma. The third condition is the diffraction requirement that the main part (for example, as defined by the first diffraction minimum) of the beam has to have an angle of propagation α that is less than the angle α_0 of total reflection. These three conditions are sufficient to calculate the threshold.

A Gaussian density profile including the refractive index $\tilde{n}$ is described by the transverse amplitudes of the electric and magnetic fields E_y and H_z:

$$\bar{E}_y^2 = \frac{e_v^2}{2|\tilde{n}|}\exp\left(-\frac{r^2}{r_0^2}\right), \qquad \bar{H}_z^2 = |\tilde{n}|^2\bar{E}_y^2. \tag{16}$$

Here, r_0 can be interpreted as the radius of the laser beam. This is only an approximation of the exact Maxwellian formulation (Cicchitelchi *et al.* 1990). The nonlinear force in the direction of r is from equations (5a) and (5b), using equation (16) (Hora 1969a) with a maximum value

$$\mathbf{f}_{NL} = \mathbf{i}_y\,\frac{1 + \tilde{n}^2E_y^2}{16\pi\tilde{n}}\,\frac{E_y^2}{r_0}\,\sqrt{2}\exp\left(-\frac{1}{2}\right). \tag{17}$$

If this has to be compensated for by a thermokinetic force under the assumption of a spatially constant plasma temperature T_{th}, we find

$$\mathbf{f}_{th} = -\mathbf{i}_y kT_{th}\left(1 + \frac{1}{Z}\right)\frac{dn_e}{dr}. \tag{18}$$

Equating this force and the nonlinear force of equation (17) provides an expression for the gradient of the plasma electron density n_e at the laser beam,

$$\frac{\partial n_e}{\partial y} = \frac{[2/\exp(1)]^{1/2}}{16\pi kT_{th}}\,(1 + |\tilde{n}|^2)\,\frac{E_v^2}{y_0|\tilde{n}|(1 + 1/Z)}. \tag{19}$$

Downloaded from https://www.cambridge.org/core. University of Basel Library, on 11 Jul 2017 at 11:30:36, subject to the Cambridge Core terms of use, available at https://www.cambridge.org/core/terms. https://doi.org/10.1017/S0263034600010119

The second physical condition of total reflection is given by the refractive index in the center of the beam $\tilde{n}$ and its value at y_0, for which with equation (19) the following expression is formulated (Hora 1969a):

$$\sin\left(\frac{\pi}{2} - \alpha_0\right) = \frac{|\tilde{n}|}{|\tilde{n}_{y0}|}. \tag{20}$$

Using a Taylor expansion and a negligibly small collision frequency leads to

$$\sin(\alpha_0) = \left(\frac{2}{\tilde{n}} \frac{\partial \tilde{n}}{\partial n_e} \frac{\partial n_e}{\partial r} r_0\right)^{1/2}. \tag{21}$$

If—as a third physical condition—a particular wave with an angle α for the first minimum of diffraction including Rayleigh's factor 1.22 has to be reflected totally, the following condition is found:

$$\sin \alpha = \frac{1.22\pi c}{2\omega r_0} \leq \sin \alpha_0. \tag{22}$$

Expressing the right-hand side by equation (21) and using equation (19) and the value of the electrical laser field amplitude E_{vo} by the averaged laser power P, a laser power threshold

$$P \geq \frac{(\pi c)^2 n^3 m_e}{e^2[2/\exp(+1)]^{1/2} c_1^2 (1 + n^2)} \tag{23}$$

is obtained, with P in watts and T in electronvolts:

$$P \geq \begin{cases} 1 \cdot 10^6 T^{-5/4} & \text{for } \omega_p \leq \omega \\ 8 \cdot 10^3 T & \text{for } \omega_p \ll \omega. \end{cases} \tag{24}$$

This was the first quantitative theory of the nonlinear force self-focusing or, as it was initially called (Hora 1969a), the ponderomotive self-focusing. This result was rederived by several other authors (Palmer 1971; Shearer *et al.* 1973) and fully reproduced. The same thresholds also are achieved by Chen's (1914) nonlinear force treatment of the filamentation instability.

A further surprising result is the fact that the power threshold for self-focusing in plasma is very low, in the range of megawatts or less. This is in agreement with measurements first published by Korobkin and Alcock (1969). Measurements of Richardson *et al.* (1971) especially demonstrated in detail that the beam center shows a depletion of plasma. Another success of the theory is the agreement of the measured beam diameters (Korobkin *et al.* 1969) of a few micrometers for a laser power of 3 MW. If one can assume that the stationary conditions for self-focusing are reached when all of the plasma is moved out of the center of the laser beam, the electromagnetic energy density $(E^2 + H^2)/8\pi$ with the electric and laser fields E and H then is equal to the cut-off density, where the laser intensity is equal to the threshold intensity I^* of the dominance of the nonlinear force. It is evident that the beam then has to shrink down to such a diameter to reach the necessary 10^{14} W/cm^2 from a laser power of 3 MW. The resulting beam diameter is then a few micrometers for neodymium glass laser radiation, in full agreement with the measurements (Korobkin *et al.* 1969).

This result was the first clarification of the kiloelectronvolt ion generation, Linlor effect (see Section 3), where (figure 4), for laser powers below 100 kW to 1 MW, the laser light always produced a classical heating, evaporation, and plasma generation, with typical tem-

Downloaded from https://www.cambridge.org/core. University of Basel Library, on 11 Jul 2017 at 11:30:36, subject to the Cambridge Core terms of use, available at https://www.cambridge.org/core/terms. https://doi.org/10.1017/S0263034600010119

peratures of 20,000 to 50,000 K and with energies of the emitted ions up to about 10 eV and an electron emission with classical Langmuir–Child space-charge limitation. Contrary to this classical behavior, laser powers above megawatt resulted in maximum kiloelectronvolt ion energies, their linear Z-dependence, and in electron emission with many orders of magnitude of higher current densities. It was concluded that, for the laser powers above megawatt, self-focusing is produced. The electromagnetic energy density in the filaments corresponds to intensities above the threshold where the nonlinear force dominates over the thermal forces, and the nonlinear force produces Z-dependence of the energetic ions from equation (14), which are given by the maximum of the swelled quiver motion

$$\epsilon_{ion} = \frac{Z}{2}\,\epsilon_{osc,\max}. \tag{25}$$

This result [Hora 1991, Eq. (9.25)] can be explained by the quiver drift of the electrons in the laser field when moving from the filament toward the incident laser beam.

While these pondermotive self-focusing mechanisms could explain the MW laser pulse threshold of the nonlinear mechanisms as kiloelectronvolt ions and linear Z-dependence, another self-focusing mechanism occurs at much higher laser intensities. It is connected with the range where the quiver motion of the electrons in the laser field reaches oscillation energies in the range of mc^2. It was shown in several examples that ion energies from 100 keV to a few hundred MeV could be well explained by this mechanism (Hora 1975).

The relativistic change of the electron mass due to oscillation energies close to or above m_0c^2 [equation (7)] causes a modification of the optical constants, as is shown in equations (2)–(4). With this relativistic intensity dependence of the absolute value of the refractive index $|\tilde{n}|$, the effective wavelength of propagating laser radiation in a plasma then is given by

$$\lambda = \frac{\lambda_0}{|\tilde{n}(I)|}, \tag{26}$$

where λ_0 is the vacuum wavelength. In figure 8, a Gaussian-like intensity profile of a laser beam moving through a homogeneous plasma is considered. The relativistic refractive index results in the condition

$$|\tilde{n}(I_{\max})| > |\tilde{n}(I_{\max}/2)|, \tag{27}$$

showing that the effective wavelength (26) is shorter for the higher laser intensity in the center of the beam than at the lower intensity of the half-maximum intensity value. As is shown in figure 8, an initially plane-wave front then is bent into a concave front, which tends to shrink down to a diffraction-limited beam diameter of about one wavelength. From the geometry of figure 8, this shrinking can be approximated by an arc resulting in a self-focusing length l_{SF}:

$$l_{SF} = \left[d_0\left(\rho_0 + \frac{d_0}{4}\right)\right]^{1/2}, \tag{28}$$

where d_0 is the initial beam diameter, and the radius of the arc with p_0 is given by the effective wavelengths of the various intensities. Also from the geometry of figure 8, the following relation is derived:

$$\frac{|\tilde{n}(I_{\max}/2)|^{-1}}{(d_0/2 + \rho_0)} = \frac{|\tilde{n}(I_{\max})|^{-1}}{\rho_0}. \tag{29}$$

Downloaded from https://www.cambridge.org/core. University of Basel Library, on 11 Jul 2017 at 11:30:36, subject to the Cambridge Core terms of use, available at https://www.cambridge.org/core/terms. https://doi.org/10.1017/S0263034600010119

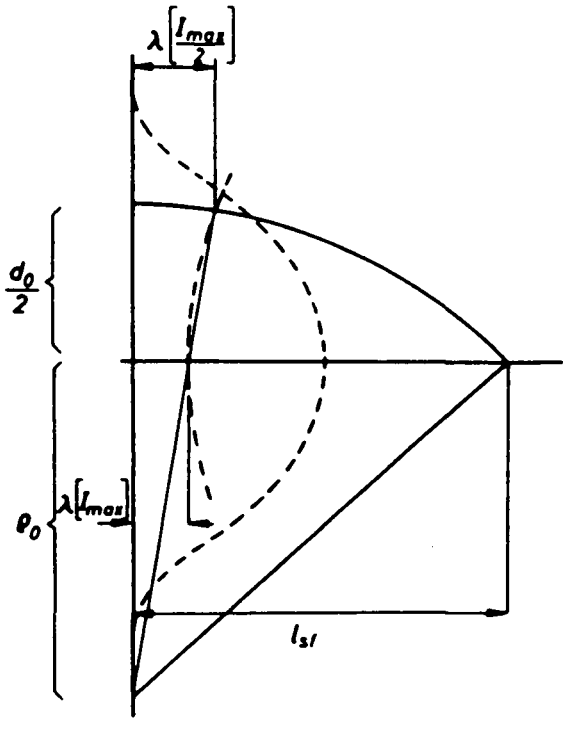

FIGURE 8. Relativistic self-focusing. Geometry of a plane-wave front (vertical line) bent into the spherical (dashed) wave front owing to the relativistic mass dependence of the refractive index at various laser intensities (Hora 1975, 1991).

In combination with equation (28), this results in the ratio of the self-focusing length related to the beam diameter (Hora 1975):

$$\frac{l_{SF}}{d_0} = 0.5\left(\frac{|\tilde{n}(I_{\max})| + |\tilde{n}(I_{\max}/2)|}{|\tilde{n}(I_{\max})| - |\tilde{n}(I_{max}/2)|}\right)^{1/2}. \tag{30}$$

Using the relativistically exact absolute value of the refractive index $\tilde{n}$ with the intensity-dependent relativistic values of the plasma frequency and the collision frequency, a numerical evaluation of equation (30) is given in figure 9 for neodymium glass laser radiation for plasma densities $N = 0.1$ or 1.0 times the nonrelativistic cut-off density value (Hora *et al.* 1977). It is remarkable that the self-focusing length is as low as two times the beam diameter for 100% of the cut-off density if the laser intensity is between 10^{16} and 3×10^{18} W/cm^2. The last intensity is the relativistic threshold corresponding to an electron oscillation energy of $m_e c^2$. It is further interesting to note that the process of the relativistic self-focusing also occurs for laser intensities that are much less than the relativistic threshold, even as much as 1000 times less. This phenomenon of the occurrence of relativistic effects at intensities much lower than the relativistic threshold was not new, as could be seen from the work concerning relativistic instabilities in plasmas (Hora 1991).

The relativistic self-focusing can be related to the generation of a Schrödinger soliton (Häuser *et al.* 1988, 1992). The subsequent acceleration of the ions in the focus will result in a smaller number of the most energetic ions in the axial direction than in the radial direc-

Downloaded from https://www.cambridge.org/core. University of Basel Library, on 11 Jul 2017 at 11:30:36, subject to the Cambridge Core terms of use, available at https://www.cambridge.org/core/terms. https://doi.org/10.1017/S0263034600010119

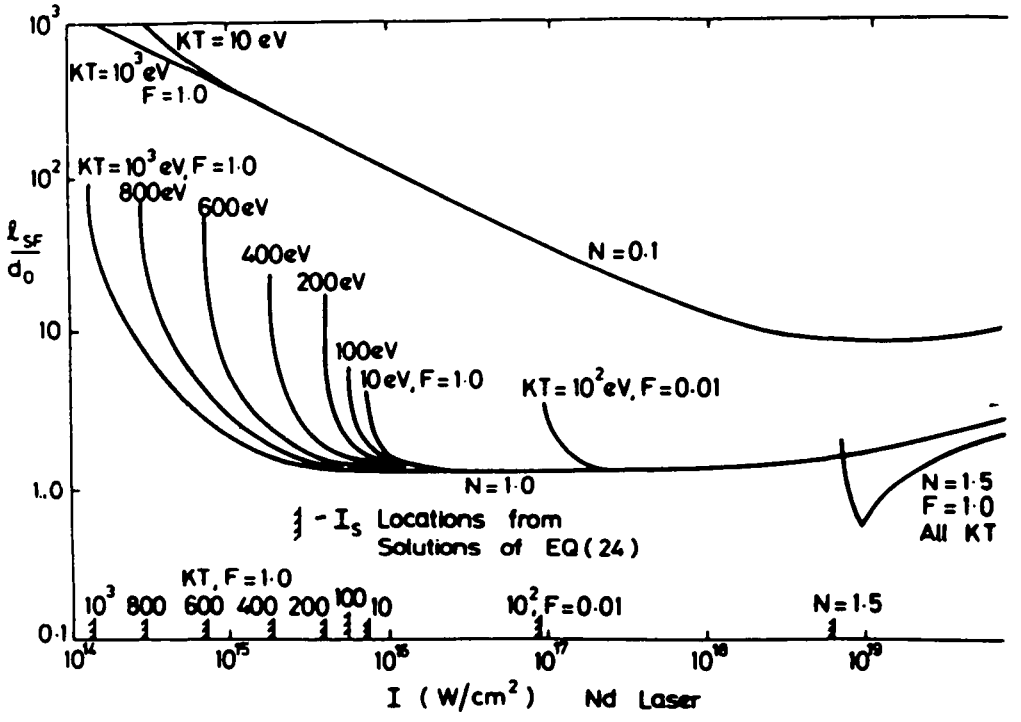

FIGURE 9. Relativistic self-focusing length l_{SF} per initial neodymium glass laser intensities I of a beam diameter d_0 for critical electron density $N = 1$ and ten times less density $N = 0.1$ for different plasma temperatures T (Hora *et al.* 1977; Kane *et al.* 1979).

tion of the focus (Häuser *et al.* 1992). This fact was observed when the ions accelerated in a laser focus at relativistic self-focusing were measured in the place of their generation (contrary to the usual time-of-flight measurement) from the Doppler shift of the X-ray spectra of 1 to 6 Å wavelength. The P^{13+} ions of 2-MeV energy from irradiation of 2×10^{15} W/cm^2 neodymium glass laser pulses corresponded to the energies expected from the relativistic self-focusing (see figure 9), but showed (from the evaluation of the absolute values of the X-ray intensity) the preferential direction of the number of emitted ions along the radius (Rode 1983; Basov *et al.* 1986) as calculated (Häuser *et al.* 1992).

The maximum ion energy is given by the simple relation [Hora 1991, Eq. (12.54)]:

$$\epsilon_i^{trans} = \tfrac{3}{4} m_e c^2 I/I_{rel} = 8.13ZP \quad \text{MeV}, \qquad [\text{P}] \text{ in TW}, \tag{31}$$

where the diameter of the focused beam, which was not determined theoretically (because of the paraxial approximation not fully reproducing the diffraction), was assumed to be twice the wavelength. The resulting ion energies between 0.1 and 500 MeV (Begay *et al.* 1983) and the corresponding measurements agree very well (see figure 10). If the experimental calibration of the X-ray spectroscopial measurements of Rode (1983) and Basov *et al.* (1986) had been used, a semiempirical determination of the diameter of the filament that was not determined theoretically at relativistic self-focusing would have been achieved, resulting in a 0.6 time smaller diameter.

The value of the ion energy of 400 MeV, taken from the result (Begay *et al.* 1983) of figure 2, agrees with the prediction of equation (31). In order to predict the maximum ion energy, if relativistic self-focusing of a kind of ANTARES laser beam of 80 TW power had

Downloaded from https://www.cambridge.org/core. University of Basel Library, on 11 Jul 2017 at 11:30:36, subject to the Cambridge Core terms of use, available at https://www.cambridge.org/core/terms. https://doi.org/10.1017/S0263034600010119

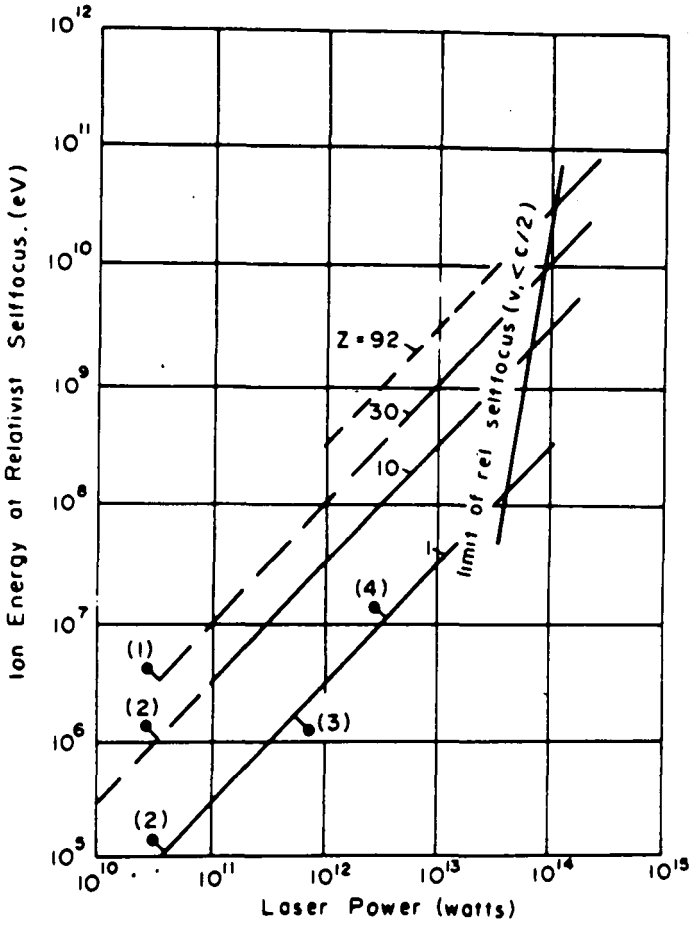

FIGURE 10. Fastest ion energies from laser-produced plasmas after relativistic self-focusing [equation (31)] (Hora 1991).

been applied, it would have been worthwhile to establish a 2D computation (Jones *et al.* 1982; Häuser *et al.* 1992) of a beam in plasma of nearly critical density. If the neodymium glass laser pulse had a rise time of 18 ps, no relativistic self-focusing would have occurred, because the radial nonlinear force was moving out of the plasma too fast before the otherwise instantly working self-focusing could be observed. Only if neodymium glass laser pulses in the terawatt range of 15 ps rise time were used would the relativistic self-focusing be fast enough compared with the expelling of the plasma from the beam. This can be seen from the temporal development of the beam radius for various depths (figure 11a), where the printout of the density profile (initially constant) at various times shows self-focusing. One example is given in figure 11b. The energy gained in the motion against the laser light in the beam axis reached 6 GeV for Sn^{38+} in agreement with the measured 6 GeV (Gitomer, 1984). This value, corresponding to equation (31), indicates that the filament diameter of the relativistically focused beam is smaller by about a factor of 2 than that which is assumed in equation (31).

It has to be underlined that the reader should keep in mind the different regimes of the nonlinear force (ponderomotive) self-focusing and the relativistic self-focusing. In the following figures 15 and 20, are the conditions of low laser intensities where nonlinear force

Downloaded from https://www.cambridge.org/core. University of Basel Library, on 11 Jul 2017 at 11:30:36, subject to the Cambridge Core terms of use, available at https://www.cambridge.org/core/terms. https://doi.org/10.1017/S0263034600010119

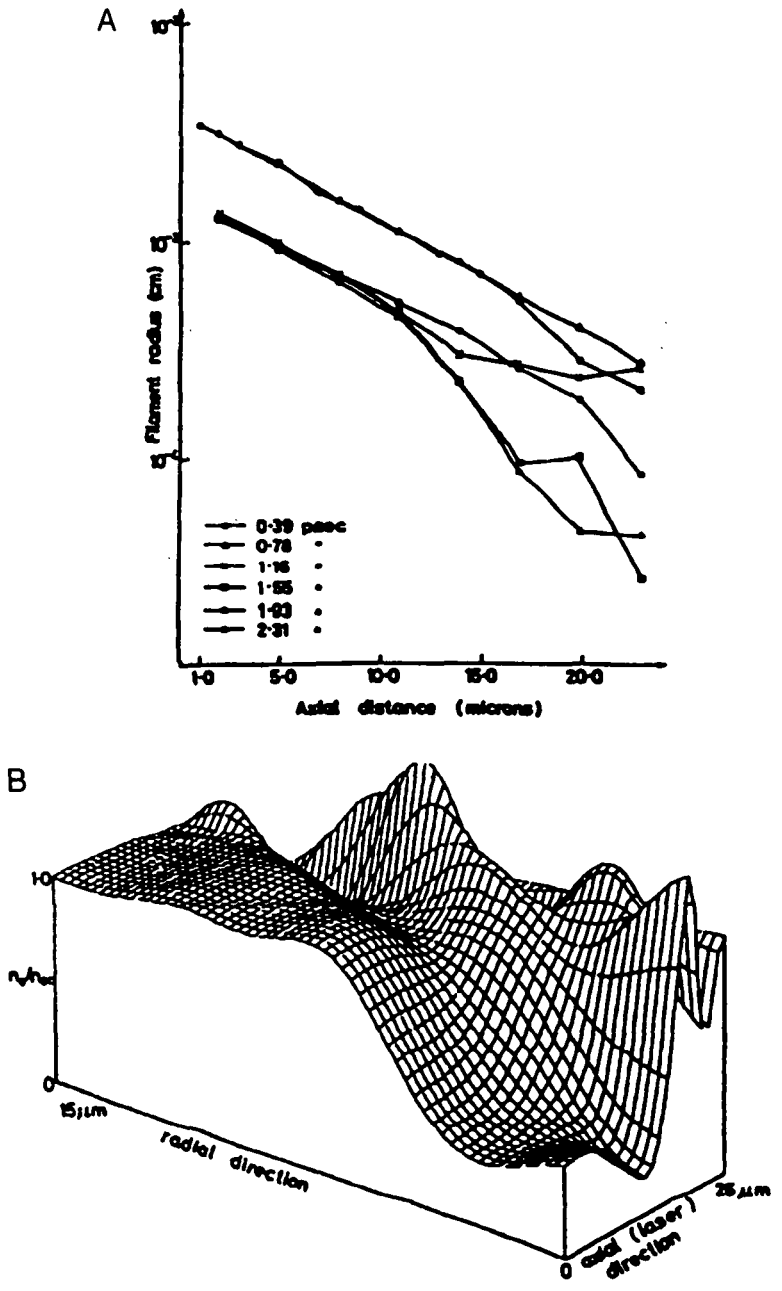

FIGURE 11. (a) A 10-TW neodymium glass laser pulse incident from the left-hand side on a Sn38+ plasma of initially uniform critical electron density. Evaluating the beam diameter over the depth for various times shows the relativistic self-focusing to one-wavelength beam diameter after 2.3 ps (Jones *et al.* 1982). (b) Same case as part (a): The initially constant critical density has been changed to the shown profile depending on the axial depth and radius at 1.16 ps (Jones *et al.* 1982; Hora 1991).

self-focusing appears, while the relativistic self-focusing of equation (31) applies only for intensities exceeding one one-thousandth of the relativistic threshold. The confusion may come from the fact that both cases separate the ions linearly by the charge number Z of the ions, a phenomenon that immediately indicates the action of the nonlinear force and

Downloaded from https://www.cambridge.org/core. University of Basel Library, on 11 Jul 2017 at 11:30:36, subject to the Cambridge Core terms of use, available at https://www.cambridge.org/core/terms. https://doi.org/10.1017/S0263034600010119

excludes any gas-dynamic acceleration mechanism. It should be mentioned that even with laser pulses of some mJ energy only, the thresholds for nonlinear force versus relativistic self-focusing come very close if ns and ps laser pulses are compared, as can be seen from ophthalmological measurements (R.H. Hora *et al.* 1992).

5. Suprathermal "hot" electrons and resonances

Analysis of the spectrum of the X-rays from laser-produced plasmas at the beginning of the 1970s produced highly confusing results. There were indications from some authors that the emitted bremsstrahlung corresponds to a temperature of about 100 eV, agreeing with gas dynamics, and there were other clear measurements of temperatures of 20 keV. A clarification was achieved by Eidmann (Büchl *et al.* 1972), whose motivation to study the laser-produced plasmas was—as it should be noted—given by Wilhelm Walcher for application as a laser ion source. Eidmann discovered that the X-ray spectrum for a large number of frequencies could be separated into a lower temperature, corresponding to the thermal electrons, and into an elevated temperature, corresponding to the energetic or "hot" electrons.

This result was confirmed repeatedly. Again, an $I\lambda^2$ relation was confirmed (Gitomer *et al.* 1986), and there exist numerous qualitative suggestions as to the reason for the energetic electrons. The dielectric swelling of the oscillation energy ϵ_{osc} within the plasma of a refractive index $\tilde{n}$ is given by equation (12) over its vacuum value (indicated by the index *vac*). The absolute value of the refractive index $\tilde{n}$ has its minimum at the critical density (where $\omega = \omega_p$), arriving then at maximum oscillation energies in the plasma. This value occurred in general hydrodynamic computations given by a swelling factor $1/\tilde{n}$ of 100 or in experiments with microwaves at 600 (Wong *et al.* 1975; Stenzel 1976). These values would be quite sufficient to explain most of the experiments (Hora 1991) of energetic electrons.

But other models appeared for the explanation of the energetic electrons. One is the Försterling–Denisov resonance absorption (Hora 1991, Chap. 12), of which the result of Maki (Hora 1991) was most convincing: If the fast thermal electrons of a Maxwellian distribution move through the very thin area of the Försterling–Denisov resonance maximum for obliquely incident laser radiation for *p*-polarization, they can be speeded up to reach the high velocities measured in the X-ray spectrum or measured directly as the emission of energetic electrons.

The Försterling–Denisov resonance absorption (Försterling 1950; Denisov 1959) appears as a very strong longitudinal oscillation of the electrons in the plasma at the critical density when the radiation is obliquely incident with *p*-polarization, with the maximum effect at an angle of incidence of about 20°. This can be seen from figure 12, where the exact Maxwellian solution of the plane-wave neodymium glass laser field obliquely incident at 26° on a plasma is evaluated. The electron density increases linearly from the vacuum value at $x = 0$ to the critical density at a depth of $x_0 = 3.14$ vacuum wavelengths. The solid line is the square of the x-component only for the electric laser field, which corresponds to a standing wave before reaching the turning point at $x_T = 2.5$ vacuum wavelengths.

Before the turning point, the laser field is that of a nearly standing wave, as is seen in the vacuum range for negative x. Within the plasma, the effective wavelength is stretched owing to the absolute value of the dielectric coefficient of less than one, and the amplitude swells in the same way and then would decay exponentially after the last standing wave maximum. The fact that the standing wave is not completely modulated is due to the absorption for the case of a plasma of 100 eV temperature. What is remarkable for the x-component of the field in the range of the exponential decay, and different from all the other components, is the appearance at very steep maximum of the resonance maximum at the critical density x_0.

Downloaded from https://www.cambridge.org/core. University of Basel Library, on 11 Jul 2017 at 11:30:36, subject to the Cambridge Core terms of use, available at https://www.cambridge.org/core/terms. https://doi.org/10.1017/S0263034600010119

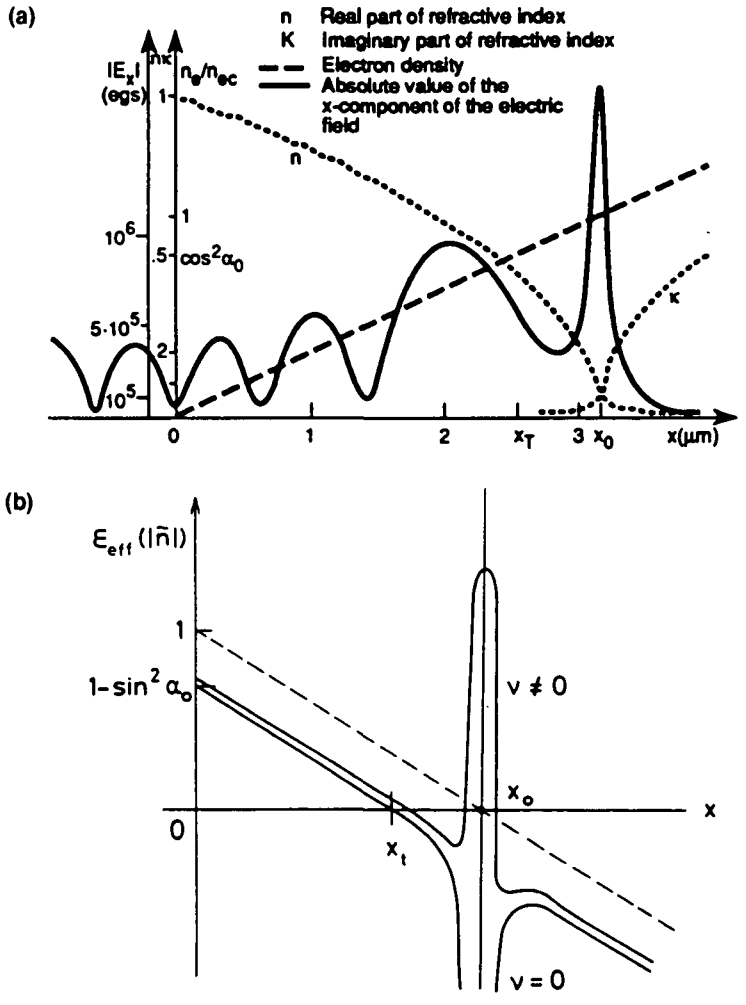

FIGURE 12. (a) Incident *p*-polarized light on 100-eV hot deuterium plasma with linear density increase along the *x*-direction. Exact Maxwellian evaluation of the *x*-component of the laser *E* field showing the exponential decay beyond the turning point x_T and a special maximum at the critical density x_0, according to Ladrach (Hora 1991). (b) The effective dielectric constant for the case in part (a) without collisions [negative pole at the critical density (White *et al.* 1974) and with collisions (high positive maximum) (Hora 1991)].

While this result is a simple linear (Airy) solution of the Maxwellian equations, where the real and imaginary parts of the refractive index are shown in figure 12a, the behavior of electrons in the neighborhood of the resonance maximum is of a nonlinear nature. One special result is the effective dielectric constant (figure 12b). For a collisionless plasma, this function has a pole of minus infinity (White *et al.* 1974) at the critical density, while adding a very tiny amount of collisions (absorption) causes the pole to jump from minus infinity to a very high positive value (Hora 1991). This is one example of how important it is to take into account the collision frequency in plasmas; otherwise, results can change from nearly plus infinity to minus infinity if the usual simplification of collisionless plasmas is assumed in the microscopic plasma theory (Hora 1991, Sec. 11.2).

Downloaded from https://www.cambridge.org/core. University of Basel Library, on 11 Jul 2017 at 11:30:36, subject to the Cambridge Core terms of use, available at https://www.cambridge.org/core/terms. https://doi.org/10.1017/S0263034600010119

The identification of the suprathermal electrons as being due to the oscillation caused by swelling was evident from the result on nonlinear force (Hora 1969, 1991). This model was favored by Brueckener, according to private discussions at the Los Alamos National Laboratory. It was shown that these electrons should not only cause the energetic X-ray signals by their oscillation, but this oscillation energy also should be converted by quiver drift into translative energy of the mentioned elevated value [Hora 1991, Eq. (11.60)]. The measurements (Ehler 1975) of the Al^{11+} ions of about 2 MeV immediately correspond to the simultaneously measured oscillation energy of 200 keV of energetic electrons in agreement with this model; see equation (14). These dielectric swelling mechanisms automatically appear in the multiparticle simulations (using one million plasma particles) (Kruer 1969), where the process of the polarization-dependent Försterling–Denisov resonance absorption and the quiver drift, as well as the internal electric fields in the plasma, also appeared automatically.

A further new resonance mechanism should be mentioned, where a similar narrow-range maximum of longitudinal oscillation in a laser-irradiated plasma is produced, as in the preceding case (figure 13), which may cause similar quiver drift energy gains of electrons. It was especially interesting to obtain therefore a resonance mechanism at perpendicular incidence of infinitely spread plane transversal electromagnetic waves on a plasma. This was in contrast with the Försterling–Denisov resonance, which appears only at obliquely incident light for *p*-polarization, and several artificial explanations were needed to discuss the related anomalous absorption mechanisms in laser-produced plasmas by assuming bent surfaces, etc.

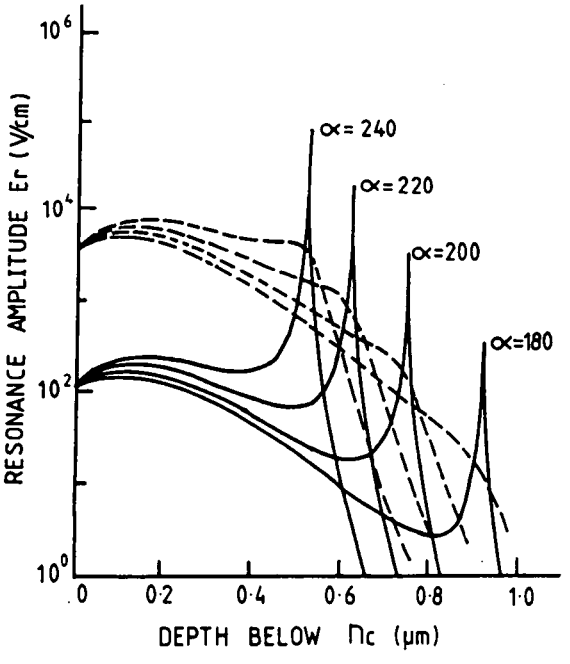

FIGURE 13. Resonance amplitude of the transverse electric field vector at perpendicular incidence on a plasma within the range of usual exponential decay beyond the critical density (new resonance), where the parameter expresses the steepness of the density profile and the dashed lines correspond to lower temperature with higher (damping) collision frequency than the other set of lines for higher temperature (Hora *et al.* 1985a; Goldsworthy *et al.* 1986).

Downloaded from https://www.cambridge.org/core. University of Basel Library, on 11 Jul 2017 at 11:30:36, subject to the Cambridge Core terms of use, available at https://www.cambridge.org/core/terms. https://doi.org/10.1017/S0263034600010119

The new resonance was found from the laser light produced by longitudinal oscillation (Hora *et al.* 1985a) of the electron gas of the plasma according to the local plasma frequency whose amplitude reaches very high values at the depth where the electron density corresponds to four times the critical density. A necessary condition is that the intensity of the laser light within this exponentially decaying area is still sufficiently large. With appropriately steep linear density profiles always occurring in Airy solutions of the Maxwellian equations, the resonance maxima can be very high and narrow (figure 13) (Goldsworthy *et al.* 1986).

The complexity of the hot electrons needs a more detailed discussion just as these aspects were brought to our attention from the studies of the energetic ion emission from targets by lasers. In the preceding two sections, we showed how the nonlinear force could explain very energetic ions and their linear separation by charges, and how self-focusing could explain how low laser powers (above the threshold of MW) could produce the necessary high laser intensities for the dominance of the nonlinear forces in the self-focusing filaments.

In this section we explained how, for example, the Försterling–Denisov resonance absorption could lead to the energetic electrons, for example, following the mechanism described by Maki *et al.* (1978) while we simultaneously underlined that this mechanism may not be dominating at all, and that other resonances and other higher harmonic generation mechanisms may be more important. We also underlined that the view of Brueckner about the quiver motion could be important for the energetic electrons. In the following we shall elaborate this proposal on the basis of a quantitative model for the anomalous resistivity.

The generation of the high X-ray emission from energetic electrons was well described numerically from one million particle simulations without collisions (Kruer 1986); from these results one at least could see how intense x-radiation may be produced even for very short laser pulses. Any quantitative formula for this process is difficult to derive from this kind of numerical studies.

It is the merit of Gitomer *et al.* (1986) that a compilation of numerous experimental results measuring the temperature T_x from X-rays due to hot electrons showed a rather good convergence; see figure 14. It is remarkable that for laser intensities (reduced to that of

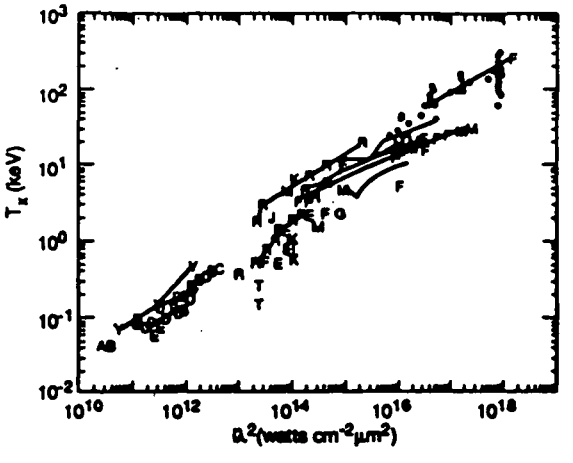

FIGURE 14. Compilation of a large number of different experiments with lasers of different wavelengths showing nearly the same measured "hot" electron temperature T_X depending on the wavelength normalized laser intensity $I\lambda^2$; from Gitomer *et al.* (1986).

Downloaded from https://www.cambridge.org/core. University of Basel Library, on 11 Jul 2017 at 11:30:36, subject to the Cambridge Core terms of use, available at https://www.cambridge.org/core/terms. https://doi.org/10.1017/S0263034600010119

neodymium glass lasers) from 10^{14} W/cm^2 up to the 10,000 times higher intensities, the empirical relation

$$T_x \sim I^{1/2} \tag{32}$$

could be derived.

The part of this hot temperature compared to the normal plasma temperature is obviously very important for laser intensities close to the relativistic threshold [equation (7)] if the laser pulses are of sufficiently long duration. It is well known that then the plasma produced from the target completely disintegrated with the emission of intense and nearly relativistic electrons such that the work with the carbon-dioxide laser ANTARES for fusion purposes was given up. The same thing happens when using shorter wavelengths if one reaches relativistic quiver energies. One exception only appears if the laser pulses are very short, for example, 100 fs for neodymium glass lasers or 1 ps for carbon-dioxide lasers: The mentioned disintegration process stops, and the total emission of X-radiation is reduced but other phenomena occur as the emission of the 111th harmonics and others appear (Joshi *et al.* 1995).

The measurements of the very energetic ions (Ehler 1975; Begay *et al.* 1983) resulted in three groups of energetic ions. The fastest group with the 0.4-TeV energy and with full linear separation depending on the ion charge may be explained easily by the relativistic self-focusing and subsequent acceleration by the nonlinear force. The slowest group is simply thermal, and the second fast group with no obvious ion separation according to their charge number, may be due to the hot electrons for which we may give the following quantitative model based on our formulation of the anomalous resistivity (Hora 1981, 1991).

The quiver motion of the electrons or the longitudinal (Langmuir) oscillation driven by the laser field with about ten times less amplitude of the longitudinal field as seen from the genuine two fluid model (Lalousis *et al.* 1982; Hora 1991) may be detected directly from the emitted radiation (Drake 1994), where the polarization dependence immediately could lead to information about the entire oscillation. Energy for the hot electrons may be considered as that which goes into the electron gas by collisions during the quiver process. This temperature T_x is (next to the usual equilibrium electron and ion temperature of the plasma) to be thermalized only later in a long-time equipartition process. The hot temperature that is received by the electron gas during a laser pulse of duration τ_L then is given by

$$T_x = \begin{cases} \dfrac{\varepsilon_{osc}\tau_L\nu}{2}, & \text{if } \tau_L\nu \le 1 \\ \dfrac{\varepsilon_{osc}}{2}, & \text{if } \tau_L\nu \ge 1, \end{cases} \tag{33}$$

where the factor 1/2 is due to the fact that only one-half of the oscillation energy [equations (7) and (12)] is the average kinetic energy. The collision frequency ν has not been taken in Spitzer's formulation (4) since the coherent quivering excludes electron–electron collisions. Therefore, for the classical case we have to use the value of the 90° scattering

$$\nu = \frac{Zn_e\pi e^4}{3^{3/2}m^{1/2}(kT)^{3/2}} = 5.229\cdot 10^{-7}\,\frac{n_e}{T^{3/2}}, \tag{34}$$

where the electron density n_e is in cm^{-3} and the temperature is in eV (see Eq. 2.34 of Hora, 1991). This collision frequency is valid only for low temperatures since for higher temperatures, instead of the 90° scattering one has to take the quantum diffraction as first derived by Marshak (1941) and formulated in a combined expression (Hora 1991, Eq. 2.50)

Downloaded from https://www.cambridge.org/core. University of Basel Library, on 11 Jul 2017 at 11:30:36, subject to the Cambridge Core terms of use, available at https://www.cambridge.org/core/terms. https://doi.org/10.1017/S0263034600010119

$$\nu_1 = \begin{cases} \dfrac{\pi r_{Bohr}^2 n_e}{4Z^3}\sqrt{\dfrac{3kT}{m}}\,[(1+4T/T^*)^{1/2}-1]^{-2}, & \text{if } T \ll T^* \\ \dfrac{\pi k^2}{3^{1/2}Zm^{3/2}}\,\dfrac{n_e}{(kT)^{1/2}} = \nu\,\dfrac{T}{T^*}, & \text{if } T \gg T^*, \end{cases} \tag{35}$$

where the temperature for separating the ranges is

$$T^* = \frac{4Z^2mc^2\alpha^2}{3k} = Z^2 36 \text{ eV} \tag{36}$$

using Planck's constant h, the fine structure constant $\alpha = 2\pi e^2/hc$, and the Bohr radius $r_{Bohr} = h^2/4\pi^2 me^2$. One sees that the collision frequency is higher than the classical at high plasma temperatures. This explains why the diffusion in a deuterium stellarator at 800 eV is measured to be 20 times faster than the classical (Hora 1991) and why the tokamak only works due to this quantum correction of the collisions, that is, due to this anomalous resistivity.

For our case of quiver motion, the plasma temperature T has to be substituted by one-half of the oscillation energy (7) such that for the high laser intensities the collision frequency in (33) is (in the nonrelativistic case)

$$\nu_1 \sim \frac{1}{\epsilon_{osc}^{1/2}} \sim \frac{1}{I^{1/2}} \tag{37}$$

or, with equation (33),

$$T_x = const\ \tau_L I^{1/2}, \tag{38}$$

in agreement with the results of Gitomer *et al.* [1986, eq. (32)] if one—for the various cases compared—could assume nearly the same laser interaction time τ_L. This could be experimentally reasonable, but it may even be experimentally exact if the stuttering (stochastic pulsation) of the laser-plasma interaction without good smoothing (Section 8) is taken into account. A deviation of the results of Gitomer *et al.* of figure 14 is possible only if good smoothing is applied, where then the laser pulse length is effective.

Equation (38) indicates that for very short pulses τ_L (<1 ps for Nd: glass lasers or <10 ps for CO_2 lasers) at the same intensity I, the ("hot" electron) temperature T_x should decrease proportional to the decreasing τ_L. This result explains why the energy of the hot electrons is very low for very short (fs) laser pulses. It is a further confirmation for the anomalous absorption—quantitatively formulated as a quantum effect in equation (35) for high quiver energies. The classical collision frequency would have resulted in

$$T_x \sim I^{-1/2}, \tag{39}$$

contrary to the observations of figure 14.

This treatment clarifies why the second fastest ion groups in the MeV ion experiments were really due to the hot electron mechanisms without charge-Z separation, contrary to the fastest 0.4-GeV ions with linear charge separation (Begay *et al.* 1983). The further argument that the fastest ions are due to the explained relativistic self-focusing and nonlinear-force acceleration mechanism can be seen from the fact (Rode 1984; Basov *et al.* 1986) that the highest charged MeV ions emitted from the laser-irradiated plasma have a strong radial preferential direction in agreement with the theory (Häuser *et al.* 1992) that anisotropy never could be explained by an isotropic "hot" electron mechanism.

We add here the observation of the linear Z-dependence observed at specific laser ion source experiments (Henkelmann *et al.* 1991) (figure 15). This again, at a much lower laser

Downloaded from https://www.cambridge.org/core. University of Basel Library, on 11 Jul 2017 at 11:30:36, subject to the Cambridge Core terms of use, available at https://www.cambridge.org/core/terms. https://doi.org/10.1017/S0263034600010119

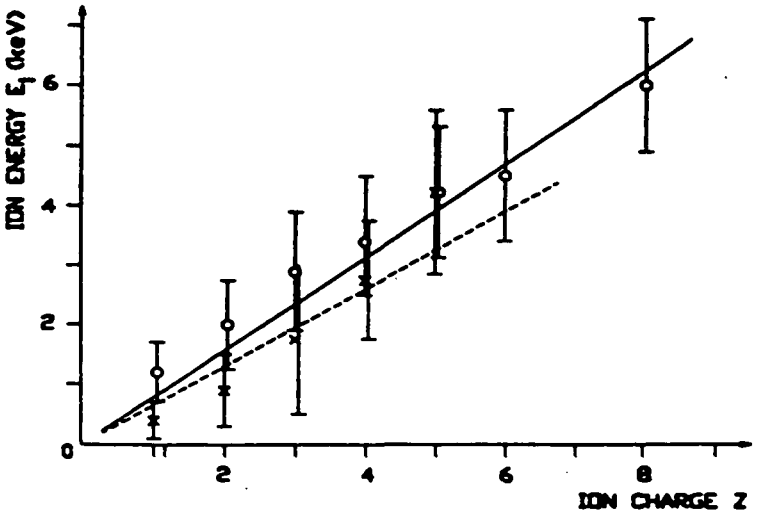

FIGURE 15. Kiloelectronvolt ions of various charge numbers Z measured for a tantalum target irradiated with 30-ps pulses at the same diameter of focus with fundamental neodymium glass wavelength and 135-mJ pulse energy (o) and 30-mJ frequency doubled laser pulses (x) (Henkelmann *et al.* 1991, 1992; Korschinek *et al.* 1991; Hora *et al.* 1992).

power, indicates the self-focusing to very high laser intensities and subsequent nonlinear force acceleration with charge separation.

6. Parametric instabilities

Referring to the two types of resonance conditions of laser interaction with plasma explained in Section 5, there is another energy transfer of laser radiation to plasma by nearly resonance conditions as known from parametric oscillations and instabilities. These parametric instabilities consist of a number of energy-transfer processes into oscillation or wave modes of the plasma with subsequent significant phenomena. One of these mechanisms is the generation of second harmonics or of 3/2 harmonics, which provides interesting information for the diagnostics of the interaction. However, it should be underlined from the beginning that it has been shown experimentally, after very extensive studies of these instability phenomena, that their net contribution to the amount of transfer for the laser energy to the plasma is not significant (Hora 1991).

The basic phenomenon "parametric instability" was called "parametric resonance" when Landau (1946) discussed an oscillating mechanical system of which one parameter was influenced by another oscillation (Spatschek 1977). One example is a mathematical pendulum of length l and mass m, whose origin oscillates in the vertical direction y by a frequency ω_0 and an amplitude A ($y = A\cos\omega_0\phi$). Using the angle ϕ as the generalized coordinate, the Lagrangian (kinetic energy minus potential energy) is then

$$L = \frac{ml^2}{2}\dot{\phi}^2 + mla\omega_0^2\cos\omega_0 t\cos\phi + mgl\cos\phi \tag{40}$$

from the Lagrange equation of the second kind

$$\frac{\partial}{\partial t}\frac{\partial}{\partial\dot{\phi}}L - \frac{\partial}{\partial\phi}L = 0, \tag{41}$$

Downloaded from https://www.cambridge.org/core. University of Basel Library, on 11 Jul 2017 at 11:30:36, subject to the Cambridge Core terms of use, available at https://www.cambridge.org/core/terms. https://doi.org/10.1017/S0263034600010119

and the following equation of motion for small amplitudes ($\sin\phi \approx \phi \ll 1$) is achieved:

$$\frac{\partial^2\phi}{\partial t^2} + [a + q\cos(\omega_0 t)]\phi = 0, \tag{42}$$

where

$$\alpha = \omega^2 \tag{43}$$

is the radian frequency of the undisturbed pendulum (amplitude of disturbance $A = 0$) and

$$q = \frac{4\omega^2 A}{l}. \tag{44}$$

Equation (42) is Mathieu's differential equation, which has the special property of quasi-periodic (stable) and nonperiodic (unstable) solutions similar to Paul's (1990) quadrupole.

The parametric instabilities in plasmas first were studied by Oraeveski and Sagdeev (1963), Silin (1965), Dubois and Goldman (1967), and Nishikawa (1968). A synopsis of all of these models was given by a treatment based on the nonlinear force (Hora 1969) presented by Chen (1974). This analysis of the parametric instabilities in plasmas at laser irradiation starts from the nonlinear force for perpendicular incidence of infinite plane waves on plasmas whose density profile permits a WKB approximation for the solution of the wave equation, equation (1),

$$\mathbf{f}_{NL} = -\mathbf{i}_x \frac{1}{16\pi}\frac{\omega_p^2}{\omega^2}\frac{\partial}{\partial x}\bar{\mathbf{E}}^2 \tag{45}$$

or

$$\mathbf{f}_{NL} = \frac{\omega_p^2}{8\pi\omega^2}\{\mathbf{E}\cdot\nabla\mathbf{E} - \mathbf{E}\times(\nabla\times\mathbf{E})\}. \tag{46}$$

Chen derived this formula from the quivering motion description (figure 1) found in most textbooks, where the difficulties due to the phase differences between **H**, **E**, and **j** (Hora 1991) were not followed up [this question was cleared up later by Kentwell *et al.* (1970)]. Chen's formulation (46) has the merit that the last term results in forces along the propagation of the laser light, while the first term works on any deviation from the striated structure in the direction perpendicular to that of the propagation. This permits us to distinguish between *backscattering instabilities*, due to $\mathbf{E}\times(\nabla\times\mathbf{E})$, and the *electrostatic parametric instabilities*, due to $\mathbf{E}\cdot\nabla\mathbf{E}$, which is equivalent to the $\mathbf{v}\cdot\nabla\mathbf{v}$ convection term in the equation of motion of this plasma. This nonlinear force in the lateral direction of the perpendicular incident plane wave may indeed need more analysis with respect to the Maxwellian stress tensor [see equation (5b)]. Chen was aware of some of these problems, and certain limitations of the following results may be necessary.

The *electrostatic parametric instabilities* are the result of the interaction of perpendicularly incident plane waves of laser radiation with the lateral deviations of n_e of the electron density from its equilibrium value n_{eo}, due to the $\mathbf{v}\cdot\nabla\mathbf{v}$ term in equation (46). For the electrostatic oscillations, the plasma frequency ω_p [equation (3)] was due to the deviation of the electrons from their equilibrium whose oscillation is attenuated by Landau damping (Biskamp *et al.* 1975). Bohm and Gross (1949) studied the generated electrostatic waves, which have the following frequency ω_e:

$$\omega_e^2 = \omega_p^2 + (3/2)k_s^2 v_{th}^2 \tag{47}$$

Downloaded from https://www.cambridge.org/core. University of Basel Library, on 11 Jul 2017 at 11:30:36, subject to the Cambridge Core terms of use, available at https://www.cambridge.org/core/terms. https://doi.org/10.1017/S0263034600010119

(Bohm–Gross frequency), where the thermal electron velocity $v_{th} = 2kT_e/m_e$ determines the transport of a signal by this wave (Langmuir wave). The wave vector k_s is given by the phase velocity v_ϕ of the wave, which can be very large:

$$|k_s| = \omega/v_\phi. \tag{48}$$

It has to be distinguished where the laser frequency ω is a little less than ω_e, in which case we have an *oscillating two-stream instability*,

$$\omega < \omega_e. \tag{49}$$

Density ripples in the direction of the electric laser field E_0 then will grow without propagation. The laterally uniform laser field E_0 then will interact with the space charge field E_1 of the density rippling by the nonlinear force $\mathbf{f}_{NL}$,

$$8\pi \frac{\omega^2}{\omega_p^2} \mathbf{f}_{NL} = -2E_0 \frac{\partial E_1}{\partial x}, \tag{50}$$

causing an increase of the ripple. A countermechanism is the stabilization of surface waves by surface tension (Eliezer *et al.* 1989).

If the laser frequency is a little higher than the Bohm–Gross frequency,

$$\omega > \omega_e, \tag{51}$$

the *parametric decay instability* is generated. The oscillating two-stream instability does not work, and the incident wave decays into an electron wave ω_e and an ion acoustic wave ω_1. The nonlinear force then acts to destroy the density perturbation n_1. However, in the frame of the moving-ion wave, the density perturbation would be at rest, as in the oscillating two-stream case. Its mechanisms again can operate based on quasineutrality and a Doppler shift, causing a growing-ion wave.

The lateral effects of the parametric decay instabilities will cause a *filamentation* or self-focusing of the laser beam in the plasma. This is based on the balance of the lateral nonlinear force with the gas-dynamic pressure as used in the earlier (Hora 1969a) treatment of self-focusing [equation (17)]:

$$\mathbf{f}_{NL} = \nabla nkT_e. \tag{52}$$

Based on a Gaussian-like density profile

$$n = n_0 \exp\left(-\frac{\omega_p^2}{\omega^2} \frac{\bar{\mathbf{E}}^2}{8\pi n_0 kT_e}\right), \tag{53}$$

a threshold for self-focusing at the laser power P_0 in watts,

$$P_0 = 8800\left(\frac{\omega_e}{\omega_p}\right)^2 T, \tag{54}$$

was found (Chen 1974), where $[T]$ = eV. This is the same value that was derived before (Hora 1969a) [equation (24)], where the mechanisms of total reflection and diffraction had been added to the balance of the forces of equation (15) only (see Section 4).

The *backscattering instabilities* occur from nonlinear forces parallel to the direction of the wave vector $\mathbf{k}$ of the laser light, where, however, the details of the quiver motion and the phases of the initial and the induced electric and magnetic fields have to be included. Again, currents and velocities are produced perpendicular to $\mathbf{k}$, reacting then with the $\mathbf{E}$ field of the laser. While the electrostatic parametric instabilities are transversing the laser

Downloaded from https://www.cambridge.org/core. University of Basel Library, on 11 Jul 2017 at 11:30:36, subject to the Cambridge Core terms of use, available at https://www.cambridge.org/core/terms. https://doi.org/10.1017/S0263034600010119

TABLE 1. Formulation of instability threshold and growth rates

	Threshold	Growth rate
SBS	$v_0^2/v_e^2 = 8y_i\nu_{ei}/\omega_i\omega_0$	$y_0 \cong (1/2)(\nu_0/c)(\omega_0/\omega_i)^{1/2}\,\omega_{pi}$
SRS	$\nu^2/c^2 = (2\omega_p^2/\omega_0^2)(y_e/\omega_p)(\nu_{ei}/\omega_0)$	$y_0 \cong (1/2)(\nu_0/c)(\omega_0\omega_p)^{1/2}$

energy into electrostatic waves, the backscatter instabilities result in a conversion into an electromagnetic wave of frequency ω nearly in or against the direction of $\mathbf{k}$. The lateral wave ω for this coupling can be equal to ω_e (an electron plasma wave); then we have *stimulated Raman scattering* (SRS). If ω is equal to that of the ion acoustic wave, we have *stimulated Brillouin scattering* (SBS). If ω is not perpendicular to $\mathbf{k}$, the density perturbation still can exist if the laser field $\mathbf{E}$ is sufficiently large to maintain it against diffusion. This then is called *resistive quasimode scattering*. If $\omega_1 = \mathbf{k}_1 * \mathbf{v}_2$ or $\mathbf{k}_1 * \mathbf{v}_i$, where $\mathbf{v}_e$ and $\mathbf{v}_i$ are the thermal velocities of electrons and ions, interaction with resonant particles can cause an instability. This is the *induced Compton scattering* or *nonlinear Landau growth*.

What is essential is that the energy balance is fulfilled,

$$\hbar\omega = \hbar\omega'_s + \hbar\omega', \tag{55}$$

where ω_s is the frequency of the scattered light and ω' is the frequency of the wave excited in the plasma, and the momentum balance is given by the corresponding wave vectors

$$\mathbf{k}_\omega = \mathbf{k}_{\omega_s} + \mathbf{k}_{\omega'}. \tag{56}$$

Without looking into the detailed derivation, the results of the threshold and growth rates in homogeneous plasma are given in table 1.

In table 1, v_e is the thermal electron velocity, y_e and y_c are the electron or ion wave damping rate, and $(\omega_p^2/\omega_0^2)(\nu_{ei}/2)$ is the damping rate of the electromagnetic waves. The threshold (Dubois 1974) for neodymium and CO_2 lasers for intensities in W/cm^2 are given in table 2.

The action of the backscatter instabilities can be seen immediately from the electromagnetic waves reflected from the laser-produced plasma. The intensity of the reflected light with half-frequency or the higher harmonics is much less than the incident light, which is the most direct indication that the instabilities do not grow to infinity, but instead are limited by saturation. The use for diagnostics is very valuable.

Since much attention has been given to parametric instabilities in laser–plasma interactions, it is necessary to consider these processes for the physics of the laser ion source. Restrictions of the described theory were caused by the fact that these models were based on homogeneous plasmas only, while extremely inhomogeneous plasmas were produced

TABLE 2. Intensity threshold for instabilities in W/cm^2

	Nd	CO_2
SBS	10^{13}	10^{10}
SRS	10^{13}	10^{9}
Oscillation two-stream instability	10^{13}	10^{9}
Parametrametric decay instability	10^{13}	10^{10}

Downloaded from https://www.cambridge.org/core. University of Basel Library, on 11 Jul 2017 at 11:30:36, subject to the Cambridge Core terms of use, available at https://www.cambridge.org/core/terms. https://doi.org/10.1017/S0263034600010119

by the laser. Apart from the mechanism of the parametric excitation of plasma oscillations (SRS) by the microscopic deviation of electron densities from equilibrium, with a definitely lower threshold for the laser intensity, there was proof of the macroscopic induction of these oscillations with very large amplitudes and without any threshold derived from the genuine two-fluid model (Eliezer *et al.* 1989, 1989a) (see Section 7).

Other limitations of the parametric instabilities have been found in experiments. Wong *et al.* (1975) and Stenzel (1976) used the small backscatter intensity as an obvious argument that the dynamics of laser–plasma interactions will not be influenced by the instabilities. This result has been confirmed theoretically by Bobin (1985), who emphasized that the parametric instabilities can work for neodymium glass lasers for intensities between 10^{14} and 10^{15} W/cm^2 only. Above these intensities, the nonlinear force is predominant for plasma dynamics. Similar conclusions were drawn by Balescu (see Hora 1991). A more detailed analysis was given by Liu *et al.* (1974), Chen *et al.* (1976), and Dragila *et al.* (1982). The nonlinear force disturbs the resonance conditions for the parametric decays. At the interesting intensities near 10^{15} W/cm^2 for neodymium glass lasers, only 1% of the absorbed radiation can go into decay modes. Under very artificial conditions, this contribution may grow to 10%.

More recent experiments elaborated these facts in more detail. It is the merit of Labaune *et al.* (1985) to have demonstrated experimentally that SBS, while really existing with all of the properties predicted theoretically, does not account very strongly for the energy transfer of laser radiation into the plasma. Only if very extreme and pathologically nonnatural density profiles with flat plateaus of 1-mm length of laser irradiation at the neodymium glass wavelength are produced artificially, is a strong amount of optical energy being transferred into the ion-acoustic waves according to SBS.

Another experimental result is that of Drake (1988), which demonstrated that SRS does not contribute a large amount of energy transfer at neodymium glass irradiation. The mechanism of SRS certainly exists with most of the theoretically predicted properties, especially the generation of the easily detectable 3/2 harmonics in backscattered light, which is due to the SRS process feeding laser energy into longitudinal electron oscillations of a frequency given by the local electron density according to the plasma frequency [equation (3)].

7. Dynamic electric fields inside plasmas and double layers causing acceleration

A rather recent development, in only the last few years, in laser-produced plasmas is to look into the problems of electric double layers and the appearance of internal electric fields that vary dynamically within the motion of inhomogeneous plasmas with or without the further modifications due to the irradiation of intense electromagnetic fields of the laser. Double layers were considered to be very marginal and usually a question that could be ignored in plasmas, while the further consequence of internal electric fields was rather a heresy in view of the space-charge neutrality of plasmas postulated in the earlier plasma physics. The space-charge neutrality (apart from the microscopic fluctuations in ranges of the Debye lengths) is indeed fulfilled if the plasma is homogeneous. This was tacitly extended to conditions of Schlüter's two-fluid model (Hora 1991), and the discrepancies should not surprise us if strongly inhomogeneous plasmas are considered. As is known from a comparable homogeneous metal, the generation of a space charge there disappears within a decay time of 0.1 fs. However, inhomogeneities lead to the contact potential or the properties of a p–n junction in semiconductors that need not be described by diffusion currents but are described much more simply as the result of static double layers and the subsequent internal electric fields.

Downloaded from https://www.cambridge.org/core. University of Basel Library, on 11 Jul 2017 at 11:30:36, subject to the Cambridge Core terms of use, available at https://www.cambridge.org/core/terms. https://doi.org/10.1017/S0263034600010119

It must be mentioned that the properties of plasma surfaces resulted in double layers and in the ambipolar fields in Langmuir's (1929) foundations of plasma physics, but this marginal question of plasmas now has turned out to be essential and of a basic nature in the inhomogeneous plasma in the universe (Alfvén 1981); it may even lead to very strong acceleration of particles, for example, in the solar corona, etc. (Fälthammer 1988). For static conditions, the double layer ideally could be studied in the triple-plasma devices (Hershkowitz 1985).

The appearance of double layers in laser-produced plasmas (Eliezer *et al.* 1989) was basically a question of the generation of energetic ions and the action of the nonlinear force. When Linlor (1963) observed the kiloelectronvolt ions suddenly appearing at laser irradiation with powers above the threshold of about 1 MW, the first idea was that the double layer at the surface may electrostatically speed up the ions to the velocity of the electrons, reaching the kiloelectronvolt ion energy from a plasma temperature of only a few electron volts. Apart from the question, why does this all not happen below the threshold of about megawatt laser power? another argument against this electrostatic acceleration as being the main reason for the kiloelectronvolt ions is the following: The double layers has the thickness of a Debye length, and the number of ions in such a volume given by the Debye length and the laser focus cross section may reach a value of only 10^9. The measurements of Linlor (1963) and all the subsequent experiments with the energetic kiloelectronvolt ions obtained four to six orders of magnitude higher numbers of ions.

This was the reason why the nonlinear force acceleration mechanism, which was derived with the linear Z-dependence of the energetic ions, needed the involvement of the ponderomotive self-focusing with a threshold of approximately megawatt power. But the electrostatic acceleration by the double layer in the plasma surface was well measured later (Wägli *et al.* 1976; Lädrach *et al.* 1979), as was proved by the identification of one group of kiloelectronvolt ions that were independent of the optical polarization. The number of such ions (Wägli *et al.* 1976) was indeed only of the order of the expected 10^9.

Apart from this very first involvement of the electric double layer in laser-produced plasmas, another impact came from the following basic question about the nonlinear force. The force density reported in Section 3 was indeed the result of the space-charge neutral theory of Schlüter, which explained that the whole plasma as a block was moved by the gradients of the electromagnetic laser field. Another model arriving at the same nonlinear forces was possible from a single-electron description. The inhomogeneous laser field caused a quiver drift of the electrons reaching the same acceleration, as is known from the nonlinear force (figure 7), except that then the inertia was not given by that of the electrons but by that of the ions [equation (14)]. This was the motivation for asking the question, in which way are high electric fields being built up when the laser takes the whole electron cloud for acceleration and the ions have to follow by field attachment? These electric fields could not be expected from Schlüter's model because such internal ones were intentionally neglected.

The way out was to develop a genuine two-fluid model for the fully ionized plasma, consisting of the electron fluid and the ion fluid between which a coupling by electrostatic fields is present. This holds in one spatial dimension only (expressed by Poissons's equation), and in three dimensions one has to add the complete Maxwellian equations obtaining them – apart from the "static" electric fields – automatically in the rather complex megagauss spontaneous magnetic fields as observed in laser-produced plasmas (Stamper *et al.* 1991). This all could be seen from an extensive numerical evaluation (Lalousis *et al.* 1983) of the motion of the coupled two fluids, for example, of a deuterium plasma in one spatial dimension for electron densities around 10^{21} cm^{-3}, corresponding to the critical cutoff density of neodymium glass laser irradiation. The numerical difficulty lies in the fact

Downloaded from https://www.cambridge.org/core. University of Basel Library, on 11 Jul 2017 at 11:30:36, subject to the Cambridge Core terms of use, available at https://www.cambridge.org/core/terms. https://doi.org/10.1017/S0263034600010119

that the temporal steps have to be 0.1 fs in order to have about ten steps per fastest plasma oscillation, while the integration of the whole dynamic system has to arrive at several picoseconds for experimental comparison. With new developments in numerical smoothing, and by the derivation of a basically new mathematical system for the solution of the initial boundary value problem (Lalousis *et al.* 1983), it was possible to solve this.

This hydrodynamic model, however, had the disadvantage that at each time step the equilibration of the energy distribution of the electrons and ions had to have Maxwellian distributions in order to follow the hydrodynamics with temperatures T of the ions and electrons. For the 1D problems there then were the seven quantities for electrons (index e) and ions (index i), the two temperatures T_i and T_e, the two densities n_i and n_e, the two velocities v_i and v_e, and the x-component, E_s, of the electric field $\mathbf{E}$, all depending on x and t to be solved by special initial and boundary values. This had to be solved by the following seven differential equations: two of continuity, two of motion, two of energy conservation, and the Poisson equation. Realistic plasmas with collisions, viscosity, and the equipartition time for temperature exchange between the two fluids were included. The transverse laser field (perpendicular to x) appeared only in the nonlinear force terms with the squares of the electric and magnetic laser fields E_L and H_L as contributions to the equation of motion of the electrons and, further, as the heat source of collisional absorption in the electron equation of energy conservation. In order to calculate the laser field from the boundary conditions of some temporal incident laser intensity, the Maxwellian equations had to be solved for the complete inhomogeneous, and dynamically developing, plasma at each time step, with the boundary condition of evanescent waves only in the superdense plasma.

This real-time realistic plasma revealed plasma properties never before obtained numerically. First—without any laser—it could be seen how a plasma expands into vacuum. Figure 16 shows the evaluated longitudinal electric field E_s between the electrons and the ions for the following initial conditions: a deuterium plasma of 1-keV electron and ion temperature with zero velocity, and a density ramp (for electrons and ions the same at the beginning) growing linearly from 5×10^{18} cm^{-3} at $x = 0$ to twice this value at $x = 10$ μm. The field is then zero at time $t = 0$. For growing time (given in periods of the smallest plasma frequency) a very hefty oscillation of the E_s field is seen. This corresponds to the fact that the electrons, with their small masses, leave the ramp very quickly by thermal hydrodynamic motion until they are stopped and returned by the E_s field. They do not return to the initial position since the ions also move hydrodynamically, owing to their temperature and the pressure gradient, and a change in the sign of the electric field does not occur anywhere. The oscillation then is damped, and after 40 periods a nearly stationary field profile is reached. The electric fields of MV/cm are to be expected, since there is a temperature of kiloelectronvolts and a plasma decay of 10^{-3} cm.

Irradiating a plasma profile with a highly bent parabolic initial density profile of 25-wavelengths thickness with neodymium glass laser radiation of 10^{17} W/cm^2 intensity, the full dynamics of laser-produced plasmas appear. The generation of the density minimum (caviton) and the speeding up of the plasma to velocities of a few 10^8 cm/s against the laser light (Eliezer *et al.* 1989; Lalousis *et al.* 1983; Hora *et al.* 1984) can be noted within 1- or 2-ps interaction (in agreement with measurements and rough hydrodynamic estimation from the magnitude of the very strongly driving nonlinear force). What can be seen, in addition, is the longitudinal electric field between the electron and ion fluid with a most complicated large amplitude (10^9-V/cm) oscillation and with the recognition of pseudo-Langmuir waves (Eliezer *et al.* 1989) (one example is given in figure 17). Owing to the caviton, an inverted double layer even appears (Hora *et al.* 1984), in agreement with measurements performed independently at the same time as the computations (Eliezer *et al.* 1989).

Downloaded from https://www.cambridge.org/core. University of Basel Library, on 11 Jul 2017 at 11:30:36, subject to the Cambridge Core terms of use, available at https://www.cambridge.org/core/terms. https://doi.org/10.1017/S0263034600010119

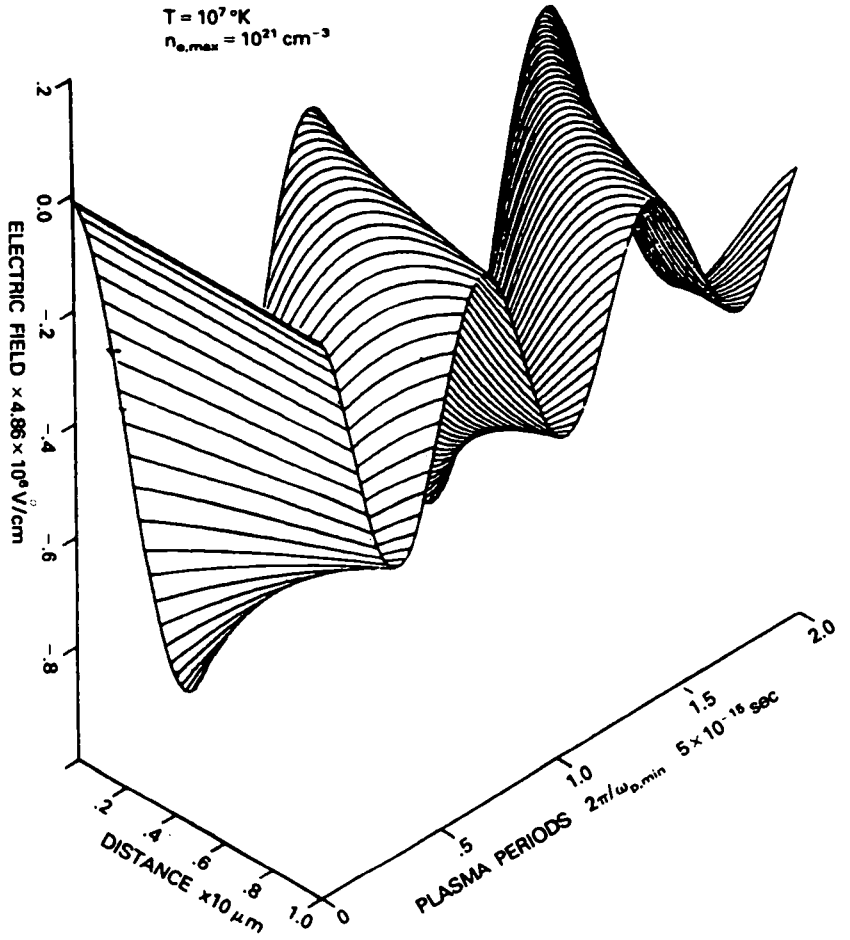

FIGURE 16. Interior electric field in the x-direction in a 1-keV temperature plasma at rest at time $t = 0$ with a density profile linearly growing along the distance $x = 0$ from 5×10^{18} cm^{-3} to twice this value at 0.01-mm depth. The electrostatically coupled motion of the electron and ion fluid at expansion shows the oscillating field (Lalousis *et al.* 1983).

It is evident that the longitudinal electric field is no longer a conservative electrostatic field. Any closed-loop path integration of this highly time-dependent $E_s(x,t)$ is then different from zero. One example of this method of energy gain and automatic acceleration of electrons within such an inhomogeneous plasma is shown in figure 18 for an initial parabolic density profile as described before (Eliezer *et al.* 1989). An electron is assumed to start to move from $x = 7$ μm against the laser light (coming from $x = 0$) with initial energies of 1, 5, and 30 keV. The energy gained by the electron during this motion is plotted in figure 18. We see that the electrons can be speeded up to 140-keV energy when leaving the plasma at the side of the laser irradiation. However, a slowing down could well occur, resulting in a motion into the reverse direction, and the 5-keV electron, for example, is then stopped at about 1.2 μm, at the time when the other electrons are leaving the plasma.

This case illustrates that it is necessary to be aware of these complex acceleration mechanisms of particles in laser-produced plasma in addition to all of the numerous mechanisms mentioned before. The double-layer mechanisms have several basic consequences, for exam-

Downloaded from https://www.cambridge.org/core. University of Basel Library, on 11 Jul 2017 at 11:30:36, subject to the Cambridge Core terms of use, available at https://www.cambridge.org/core/terms. https://doi.org/10.1017/S0263034600010119

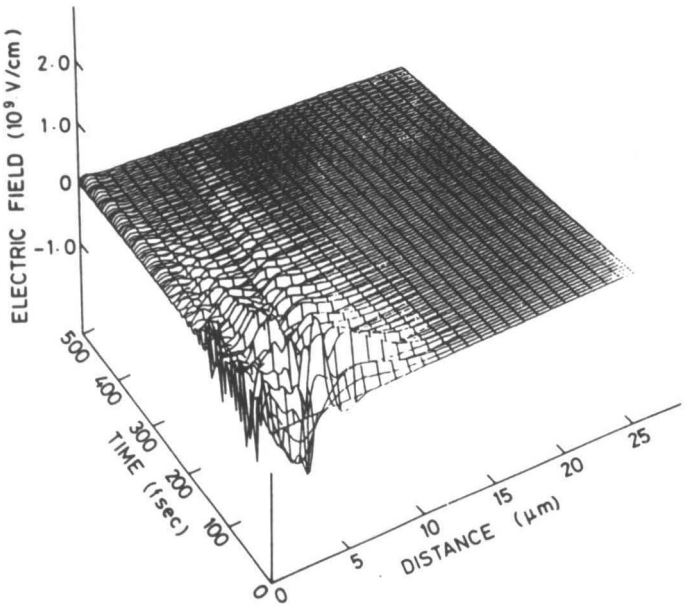

FIGURE 17. Longitudinal electric field in the plasma produced by 10^{17} W/cm^2 neodymium glass laser irradiation of a 25-wavelength-thick plasma slab of parabolic initial ($t = 0$) density (Eliezer *et al.* 1989).

ple, in stabilizing surface waves from the surface tension that is a result of the electric fields in the double layers. Even the generation of surface tension in metal can be explained by this plasma model of surface tension reproducing the measured values (Hora *et al.* 1989) (without the difficulty of negative values as known from the jellium model) in a straightforward way, when the (then-degenerate) electron gas—as in the case of a plasma—likes to leave the ions until the generated electric field produces the double layer that defines the

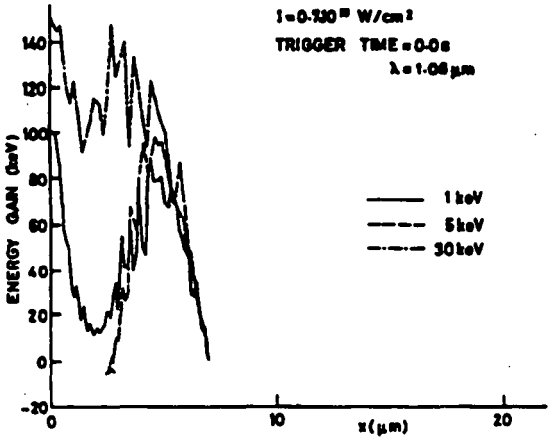

FIGURE 18. Similar to figure 17, but for seven times higher laser intensity. Electrons are moving in this dynamic field from the depth of 7 wavelengths in the plasma toward the laser light with three different initial energies. The energy gain of the electrons can be more than 140 keV owing to the laser-driven dynamic electric fields (Hora 1991).

Downloaded from https://www.cambridge.org/core. University of Basel Library, on 11 Jul 2017 at 11:30:36, subject to the Cambridge Core terms of use, available at https://www.cambridge.org/core/terms. https://doi.org/10.1017/S0263034600010119

thermionic exit potential for the electrons. While this potential is given by the Fermi energy, that of the low-density high-temperature plasma is simply given by kT.

This first derivation of surface tension of plasma due to the electrostatic energy in the double layer per surface area (Eliezer *et al.* 1989) was rather a surprise in plasma theory, because any analogy with the case of the dipole-saturation–produced surface tension in liquids cannot be applied to fully ionized plasmas. Nevertheless, there were observations in plasmas that surface tension may work. This was seen, for example, from the smooth surface of the plasma produced by lasers from a solid target. Another case is related to the field of this article: Studies of the duoplasmatron showed (Ardenne 1956) plasma generation on surfaces that evidently could be interpreted as surface tension (Langbein *et al.* 1990), although the theoretical background was not derived when this was observed.

The electric fields are therefore essential inside all inhomogeneous plasmas, and, if these move hydrodynamically, the field is a complicated spatial and temporal function. A rather general local approximation of this field is given by the following equation (Hora *et al.* 1985; Goldsworthy *et al.* 1986; Eliezer *et al.* 1989):

$$E_s = \frac{4\pi e}{\omega_p^2}\left[\frac{\partial}{\partial x}\left(\frac{3n_i kT_i}{m_i} + Zn_i \nu v_i^2\right) - \frac{\partial}{\partial x}\left(\frac{3n_e kT_e}{m_e} + Zn_e \nu_{ei}^2\right) + \frac{1}{m_e}\frac{\partial}{\partial x}\frac{(E_L^2 + H_L^2)}{8\pi}\right]\pi$$
$$\times\left[1 - \exp\left(-\frac{\nu}{2}t\right)\cos\omega_p t\right] + \frac{\omega_p^2 - 4\omega^2}{(\omega_p^2 - 4\omega^2)^2 + \nu^2\omega^2}\frac{4\pi e}{m_e}\frac{\partial}{\partial x}(E_L^2 + H_L^2)\cos 2\omega t$$
$$\times\frac{2\nu\omega}{(\omega_p^2 - 4\omega^2)^2 + \nu^2\omega^2}\frac{4\pi e}{m_e}\frac{\partial}{\partial x}(E_L^2 + H_L^2)\sin 2\omega t, \tag{57}$$

where the classical Langmuir (1929) ambipolar field as a gradient of nkT appears for the electrons. In addition to this, however, very many more terms have been derived (Eliezer *et al.* 1989), including a pressure (in the first term) given by the gradient of $E_L^2 + H_L^2$, which then can be realized not as a ponderomotive "potential" but in general as a nonconservative expression. All of these pressures, including the trivial ambipolar one (first square bracket of first term), are then not constant, as in the case of Langmuir, but (apart from a constant basis) they oscillate with the local plasma frequency damped by the collision frequency. The last term, which is important only where gradients of the laser field energy density appear, is the reason for the "new resonance" we mentioned in Section 5 (figure 13) at four times the critical density (Hora *et al.* 1985; Goldsworthy *et al.* 1986). The term before is the reason for the high-intensity second-harmonics emission of laser radiation from the irradiated plasma corona with nearly the same intensity at very low and high plasma density, and with some spatial periodicities. This unique second-harmonics emission, which cannot be understood from instabilities and anomalous resonances but simply and qualitatively reproduced from the mentioned term, has been measured by Aleksandrova *et al.* and by Gu Min *et al.* (see Hora 1991). These mechanisms should be taken into account, in addition to all of the complications of laser interaction with plasmas mentioned above, if the processes of the laser ion source are being studied.

8. Pulsating (stuttering) interaction and smoothing

We now will review a very important phenomenon that was discovered only during the last few years, but whose initial appearance goes back to the early 1970s. These results may, in retrospect, modify or complement the preceding sections, especially with respect to the energetic ion generation from self-focusing. However, most of these mechanisms now are undergoing deeper and very necessary clarification, which may have immediate consequences for studying well-defined physics questions in order to develop further the laser ion source.

Downloaded from https://www.cambridge.org/core. University of Basel Library, on 11 Jul 2017 at 11:30:36, subject to the Cambridge Core terms of use, available at https://www.cambridge.org/core/terms. https://doi.org/10.1017/S0263034600010119

The new phenomenon is the temporal pulsation of laser–plasma interaction with a fully stochastic "sequence" between 10 and 50 ps. This result was gained entirely empirically (Maddever *et al.* 1990) from a phenomenon of a spectral modulation of light reflected from laser-produced plasmas. It seems that this is a very basic phenomenon which was just not known as one—or perhaps the essential—reason for the most complicated behavior of laser-produced plasmas.

It was however well known during all of the 30 years of research on laser-produced plasmas, since the laser was discovered, that the interaction is very complex. This appeared especially with the broad stream of research on laser–plasma interactions with the aim of inertial-confinement fusion. A number of the strange observations were known as the energetic ions, or their nonlinear expansion (figure 5), or the suprathermal electrons apart from the thermal ones, and they were confirmed repeatedly before the large-scale laser fusion projects were initiated in 1972. Nevertheless, it was quite a surprise when the laser fusion experiments in the mid-1970s showed all kinds of these and other confusing anomalies, which were frustrating and delayed the hope of an easy solution of fusion energy from lasers. One way out was the indirect drive introduced by Nuckolls (1982), where the laser energy first is converted into X-rays, and the driving of the compression and heating of the fusion pellets then is done by the X-rays. These are then rather smooth compared with the direct drive interaction of the laser irradiation.

The difficulties of the laser–plasma interaction mostly were considered to be due to the parametric instabilities, such as stimulated Raman or Brillouin scattering, SRS and SBS (see Section 6). While these mechanisms are evident from diagnostics and can be used actively to determine the plasma properties, it took a long time to prove experimentally that SRS (Drake 1988) and SBS (Labaune 1985) do not dominate the energy transfer from the laser to the plasma. The question was then, what is the reason for the confusing results?

First indications go back to 1973. There were the computations of laser interactions with plasma, including the nonlinear forces as well as nonlinear optical constants with collisional absorption and including the exact Maxwellian solution of the laser field in the irradiated plasma corona. This showed temporal and spatial variation of propagating- and standing-wave field components depending on the whole plasma dynamics. Initially, the laser light penetrated up to the critical density, as expected, was reflected there and resulted in a net reflectivity of a few percent. What happened next at high laser intensities was that the nonlinear (ponderomotive) forces (Hora 1991) pushed the plasma into the nodes of the rigid standing wave of the coherent plane-wave laser field within 2 ps, and after the plasma reached a speed of a few times 10^7 cm/s within 2 ps, the generated density ripple acted as a self-produced ideal Bragg–Laue grating. This reflected the laser light by nearly 95% within the very low density in the most peripheric plasma corona [see Hora (1991, Fig. 10.10) from the computations of 1973].

Such a reflection phenomenon then was observed by Lubin (1974). In that experiment, the reflectivity of a laser-irradiated plasma oscillated irregularly from a few percent to nearly 100% and back to a few percent, etc., within 10 to 40 ps. Exactly the same pulsating reflectivity was reproduced by Maddever *et al.* (1990), and it was even confirmed experimentally that the location of the reflectivity in the case of a low percentage is at the critical plasma density, and for a high percentage of reflection it is located at the very low density of the outermost part of the plasma corona. It was observed that the plasma gets a push to the velocity of about 2×10^7 cm/s within a few picoseconds and has no acceleration until about 15 ps later, when another push comes from the laser light by a further interaction, etc. This was the long-searched-for clarification as to why the specrtrum of backscattered radiation had a spectral (stochastic) modulation of about 4 Å (Maddever *et al.* 1990), corresponding to the repeated pushing of the stepwise plasma acceleration.

Downloaded from https://www.cambridge.org/core. University of Basel Library, on 11 Jul 2017 at 11:30:36, subject to the Cambridge Core terms of use, available at https://www.cambridge.org/core/terms. https://doi.org/10.1017/S0263034600010119

This behavior could be reproduced exactly numerically from a very detailed hydrodynamic model. After the standing wave produced the density ripple, no light penetrated the corona and the ripple relaxed hydromechanically until about 8 ps later, when light again could penetrate to the critical density, again causing a density ripple, Laue reflection, stopping of the acceleration, etc. (figure 19) (Aydin *et al.* 1992; Hora *et al.* 1992). The computed velocity diagrams show similar pulsations of the velocity in steps according to the 8-ps pulsation or stuttering, but, in addition, it can be recognized that, between each of the rippling processes, the velocity at the initial point of laser incidence receives a step in the range of 10^7 cm/s, as is observed from the Doppler-modulated spectrum (Hora *et al.* 1992).

The same pulsation was observed in another experiment for the 3/2 harmonics scattering (Guilietti 1989) and for other phenomena such as the double-layer potentials or the H-α emission (Luther-Davies *et al.* 1993). The very sophisticated proof of this explanation of the pulsation can be based on experiments that were intuitively motivated, and performed many years ago—in 1973—after the computational result of the self-generated Laue grating. Putting a question mark in the laser beam (Eidmann *et al.* 1974), it was shown that it was reflected on the top, indicating that there was a phase-like reflection and no mirror-like reflection. The better resolution of the experiment (Sigel *et al.* 1976) showed, however, that the question mark jumped up and down in a period of about 25 to 30 ps. This curiosity now can be explained simply after knowing the pulsation and rippling. As long as the light with low reflectivity moves to the critical density, it is regularly mirror-reflected. When the density ripple is generated at high reflectivity every 8 to 25 ps, we expect phase reflection with the question mark on top. The repetition of this experiment with better time resolution will be most interesting, not only with respect to fusion research, but also for the laser ion source. The jumping of the question mark can be used as a test to see if there is still a stuttering or when abolishing the stuttering, as is explained in the following.

The way to solve all of these complex observations is obtained by the smoothing of the laser beam. These techniques were indeed suggested to overcome another problem (Kato *et al.* 1984). The motivation was to achieve a very lateral uniformity in the laser intensity

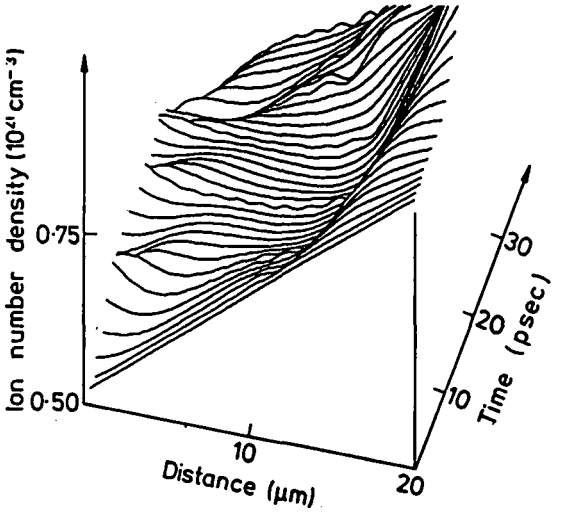

FIGURE 19. Ion density in an initial 30-eV deuterium plasma with initial linear density profile at a neodymium glass laser irradiation of 10^{15} W/cm^2 from the left-hand side developing in time using the very general real-time genuine two-fluid model, where a rippling appears nearly periodically about every 8 ps (Aydin *et al.* 1992; Horá *et al.* 1992).

Downloaded from https://www.cambridge.org/core. University of Basel Library, on 11 Jul 2017 at 11:30:36, subject to the Cambridge Core terms of use, available at https://www.cambridge.org/core/terms. https://doi.org/10.1017/S0263034600010119

across the laser beam and to avoid filamentation and self-focusing (Section 4). It was discovered empirically earlier, without knowing the details of this pulsation process. The use of the random-phase plate (Kato *et al.* 1984), or the induced spatial incoherence (ISI) (Lehmberg *et al.* 1983), or the fly-eye lens array (Deng *et al.* 1986), or the spatial spectral dispersion (Skupski *et al.* 1989) caused, for example, a coherence of the light only for 2 ps. The consequence is that the standing waves were not fixed, but washed out by the laser itself, and no Bragg–Laue grating could be generated with all of its consequences; subsequently, the pulsating 3/2 harmonics changed into a smooth emission (Giulietti *et al.* 1989) when a random-phase plane was used, or a very smooth picture of the light reflected from a target was seen with the smoothing techniques, contrary to the very granulated picture without smoothing. This smooth interaction may be the long-expected physics solution of direct-drive laser fusion (Eliezer *et al.* 1993).

For the acceleration in the laser ion source, the process of stuttering and its suppression by the smoothing may be of essential importance. This refers especially to the mechanism of self-focusing of laser beams in plasmas and whether this is the reason for an explanation of the measured kiloelectronvolt and megaelectronvolt ions (Hora 1975) (Section 4).

It was indeed known that the relativistic self-focusing (Hora 1975; Jones *et al.* 1982) needed an interaction of about 10 ps or less for neodymium glass laser pulses and 70 ps for intense carbon-dioxide laser pulses (Clark *et al.* 1985). Without the pulsation, which was detected so much later, the essential presumptions for the ponderomotive (Hora 1969a) and the relativistic self-focusing (Hora 1975) would not have been fulfilled. The result of the agreement of the models with the measurements (linear Z-dependence, result of 20-keV ions from plasma of about 100-eV temperature, isotropic generation of megaelectronvolt ion energies) was convincing, but the explanation of the pulsation was lacking.

Fortunately, there are now measurements available—which were in no way influenced by the new aspects of the pulsation—which were performed for studies of the laser ion source and may just meet the results expected for the pulsation without smoothing. The measurements (Korschinek *et al.* 1986) were performed with neodymium glass laser pulses of the fundamental frequency (red) or for the second harmonics (green) of a few mJ to 10-J energy for durations of between 30 ps and 3 ns irradiated on plane tantalum and other targets in vacuum. The merit of the long years of the project (Henkelmann *et al.* 1991; Korschinek *et al.* 1991) was not only to clarify, for the first time, many problems concerning the laser ion source with respect to the extraction of the ions from the plasma plume by electric fields and with respect to recombination, but also the large amount of very systematic measurements of ion energies, using various ion analyzers apart from the time-of-flight diagrams, should result in a large stock of empirical results for a wide range of parameters and for reliable comparisons of cases of various laser energies and intensities, various pulse duration, and for the fundamental and the double-laser frequencies.

Some remarks are necessary about the determination of the focus spot in the experiments. Its geometric extent was determined with rather low accuracy from the far-field pattern of the beam, as in the usual cases where high accuracy was not necessary. It was very important to always use the same conditions when comparing ion emission from focal spots for laser pulses of different durations and different energies. For the relative comparisons, the error of the focal dimension was compensated. The following results and their relative high accuracy of comparison are the best proof of the validity of this fact.

Figure 15 shows the energetic ion energies (keV) emitted from a tantalum target when irradiated by second-harmonics neodymium glass pulses with exactly the same focus geometry. In one case, the laser pulses are of 30-ps duration and 60-mJ energy, and in the other case their duration is 3 ns and the energy 6 J, such that, in both cases, the laser intensity is the same. What is an enormous surprise is that the ion energies depending on the ion-

Downloaded from https://www.cambridge.org/core. University of Basel Library, on 11 Jul 2017 at 11:30:36, subject to the Cambridge Core terms of use, available at https://www.cambridge.org/core/terms. https://doi.org/10.1017/S0263034600010119

ization number Z are the same in both cases, although the laser pulse energy is 100 times higher in one of the cases. It would have been expected that the 100-times higher laser energy would produce a very much higher ion energy. For the slow thermal plasma following the kiloelectronvolt ion, there is indeed a drastic difference, as was expected, and a secondary ion stripping process occurs for the long pulses with the existing high-density plasma plume in front of the target compared with the short-pulse case (Hora *et al.* 1992). There is a linear increase of the ion energy on Z—equal to the 30-ps case—up to $Z = 8$, but then the ion energy is constant.

The generation of constant-energy higher charge states in long pulses must be due to another mechanism. If the stuttering mechanism is correct, ions will have sufficiently short pulses; obviously there is only one interaction and no dense plasma cloud. It remains to be seen whether the passage of ions through the dense plasma cloud could increase their charge state without a significant change in energy.

Stripping can be excluded since ion energies above 10 MeV would be needed in solid targets, and gas or plasma targets are even less efficient. It could be asked whether electrons with energies of 100–300 eV in the plasma in front of the target could increase the charge state by electron impact ionization (EII) or related processes. The low mass of the electron would not seriously perturb the ion energy.

The total number of Ta^{q+} ions can be obtained from

$$N = nvat, \tag{58}$$

where n is the density of Ta^{q+} ions, v is their velocity, a is the average cross section of the plasma in front of the target perpendicular to the laser beam axis (10^{-3}cm^2), and t is the laser pulse duration (3 ns). The density of the Ta^{q+} ions is given by

$$n_{Ta^{q+}} = S^{EII}_{Ta^{q+}} n_e n_{Ta^{(q-1)+}} + t', \tag{59}$$

where n_e is the average electron density (assumed to be 10^{18} cm^{-3}), $na_{\text{Ta(q-1)+}}$ is the ion density in the initial charge state (e.g., $n_{\text{Ta11+}} \approx 10^{15}$ cm^{-3}), and t' is the interaction time for ions with the plasma (estimated as 0.6 ps). S^{EII} is the ionization rate obtained by folding the EII cross section σ^{EII} with the Maxwellian velocity distribution of the elements v',

$$\begin{aligned} S^{EII} &= (\sigma^{EII} v') \\ &= \sqrt{8kT/\pi m} \int_{J/kT}^{\infty} \sigma(E)(E/kT) e^{(-E/kT)} d(E/kT), \end{aligned} \tag{60}$$

where J is the ionization potential. The EII cross section for tantalum can be scaled with sufficient accuracy for this exercise from theoretical values of analogous elements (Hora *et al.* 1992). As the exact ionization potential of Ta^{11+} is not known, it is assumed to be approximately equal to the eigenvalue energy of the 4f subshell, which is 235 eV. As the average plasma temperature is of the order of a few 100 eV, electron impact ionization is highly possible. The EII cross section was evaluated using the scaling laws of a given isoelectronic series from the calculated cross section of Eu^{+} (Yonger 1987; Hora *et al.* 1992),

$$J^2 \sigma(E) = \sigma_c(X), \tag{61}$$

where $\sigma(E)$ is the cross section for an ion of ionization potential J for electron energy E, $\sigma_c(X)$ is the scaled cross section (the same for all ions in an isoelectronic sequence), and $X = E/J$. This gives an EII cross section of 4×10^{-17} cm^2 for Ta^{11+}. This value is comparable to those given empirically by the Born approximation (Mc Guire 1979), the Lotz (1967) formula, and Donets scaling from EBIS measurements (Becker 1980). This cross section gives an estimate of the number of Ta^{12+} ions produced during the laser pulse as 6×10^{11}

Downloaded from https://www.cambridge.org/core. University of Basel Library, on 11 Jul 2017 at 11:30:36, subject to the Cambridge Core terms of use, available at https://www.cambridge.org/core/terms. https://doi.org/10.1017/S0263034600010119

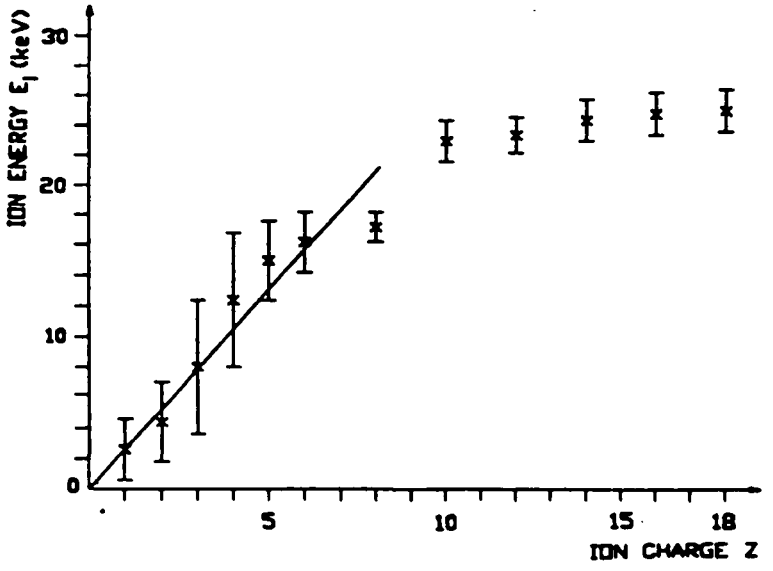

FIGURE 20. Kiloelectronvolt ions of various charge numbers Z from neodymium glass laser-irradiated tantalum at the intensity $I = 4 \times 10^{13}$ W/cm^2 for pulses of 3 ns, 6 J with comparable intensities of 30-ps pulses in figure 15 (Hora *et al.* 1992).

and would seem to indicate that the observed abundances of ions (10^{10}–10^{12}) up to 18+ (Sharkov *et al.* 1991) are within the possibilities of EII. The presence of laser radiation in the target plasma will decrease the ionization potential and modify cross sections (Chirkov 1990), but these effects would only change the number of ions slightly, which, in any case, is only an estimation.

The charge independence of ion energies (figure 20) shows that recombination and electrostatic acceleration do not influence the properties of the energetic ions. Each of these processes would modify the ion energy. Linear charge state dependence for charge states less than 10+ thus are shown to be due to the basic initial mechanism of ion generation and not by space-charge, hydromechanical, or thermal recombination processes that were claimed (but never proven). The charge state independence above 10+ follows the EII mechanism as in the ECR, however, with the very much higher ion densities produced by the laser. It also excludes thermal and electrostatic paths.

9. Consequences and possibilities of the laser ion source

The very comprehensive description of the physics of laser interaction with plasmas—in view of the whole of knowledge (mostly gained from laser fusion studies) of the field, this is still a short review—was necessary to prepare the reader to appreciate how extremely complex the physics of the laser ion source is. The first small steps in developing the laser ion source for large accelerators (see Section 2) were so very promising in obtaining at least about 100 times higher currents of ions for injection into synchrotrons than before, that they may justify more extensive consideration for the laser ion source. In addition, the experimental results of a very large transfer of optical energy into nearly megaelectronvolt highly charged ions at higher laser intensities may be another considerable advantage for the laser ion source to come, with a possible further strong increase of the ion number and very high charge state.

Downloaded from https://www.cambridge.org/core. University of Basel Library, on 11 Jul 2017 at 11:30:36, subject to the Cambridge Core terms of use, available at https://www.cambridge.org/core/terms. https://doi.org/10.1017/S0263034600010119

The extensive explanation of physics phenomena in Sections 3 to 8 contained some remarkable results for the understanding of some of the confusing experimental observations. It seems to be clarified now that the threshold of changing from the classical thermokinetic plasma behavior at laser irradiation below 1 MW to the nonclassical behavior at higher powers, with the sudden appearance of kiloelectronvolt ions, coincides with the ponderomotive self-focusing threshold (Hora 1969a), explaining the observed diameters of the filaments and the generation of optical-energy densities above the thermal ones such that the generation of the kiloelectronvolt ions and their linear separation by the ion charge Z can be explained.

It further seems to be clarified that the relativistic self-focusing, beginning at 10^{15} W/cm^2 for neodymium glass laser radiation and at a 100 times lower intensity for carbon-dioxide lasers, reaches the measured ion energies in the range of 0.1 to 500 MeV and their linear Z-dependence, as well as their preferential emission in the radial direction, as explained by a Schrödinger soliton mechanism (Häuser *et al.* 1988). A special success was the explanation of all of these measured megaelectronvolt ion energies and radial emission preferences from the X-ray spectroscopical diagnostics of Rode (1983) and Basov *et al.* (1986). Furthermore, all of the ion energies up to 400 MeV measured by different laboratories could be explained immediately by the relativistic self-focusing, and predictions to 6 GeV ion energies (measured later: Gitomer, 1984) with remarkably high current are important (Jones *et al.* 1982).

Nevertheless, these successes are only the first step. In reality, the whole physics is very complex. It is necessary not only to look at the megawatt threshold or the maximum ion energy, but also at the whole spectrum of energetic (suprathermal) ions, at their specific angular dependence, at their interaction with the neighboring plasma or target material, and last, but not least, also at the remaining thermokinetic part of plasma following the energetic part. It indeed would be naive to expect a description from a 1D gas-dynamic model to reproduce all of these phenomena, although—as shown from the central part of the plasma of figure 8—the low energy part can well be followed up by gas-dynamic models for low (i.e., below about 1 keV) temperatures and moderate laser pulse energies; and even a separation of the ions of less than 100 eV energy by their charge number may well be covered by a thermal recombination mechanism.

For an experimental research program, some significant new phenomena need to be clarified, which may be made in a punctual way, as, for example, the inclusion of the pulsating interaction (see Section 8) by using or avoiding the smoothing techniques. Another interesting point would be to study directly the self-focusing properties. The use of such clear experimental conditions, as in the work of the Korschinek (1991) group, for distinguishing the same conditions for different wavelengths, furthermore will result in numerous clarifications of several of the complex physics questions. In view of these new results, an extension of the otherwise well-developed experimental diagnostics of the emitted ions, their energy spectra, their direction dependence, their space charge, and recombination effects may be another stimulant.

Also of interest are the ion extraction mechanism and guiding into linac preaccelerators (Sharkov *et al.* 1992) or cyclotrons (figure 3), and the application of the extensive knowledge available from accelerator physics. Since there are new parameters to be treated now that were not available before, with much larger ion numbers and higher ion current densities, shorter pulses, etc., even this classical accelerator knowledge may need an extension toward space-charge effects, recombination (even three-body recombination as known from laser-produced plasmas), and problems of luminosity.

The proved success of the laser ion source, even for particular low power laser installations at Dubna (Monchinski 1991; Kutner *et al.* 1990; Barabash *et al.* 1984), at the Insti-

Downloaded from https://www.cambridge.org/core. University of Basel Library, on 11 Jul 2017 at 11:30:36, subject to the Cambridge Core terms of use, available at https://www.cambridge.org/core/terms. https://doi.org/10.1017/S0263034600010119

tute of Theoretical and Experimental Physics in Moscow (Sharkov *et al.* 1992), and at CERN (Sherwood 1995) may justify an extensive program to study specifically the physics and the engineering development of the laser ion source. In view of the fact that accelerators costing several thousand millions of dollars are involved, the use of ion (and lepton) sources, with lasers providing several orders of magnitude better ion pulses, may well justify a specific program of several million dollars. The review given in this article of the future developments of the various ion sources may support the opinion that no miracles can be expected from improvements of the existing classical plasma ion sources. On the other hand, no total guarantee can be given for the laser ion source at the moment, apart from encouraging improvement by orders of magnitude. However, the necessary development of large lasers with high repetition rates, high energies, and very high intensity pulses, has greatly matured, so that a not-too-expensive solution can be envisaged for a completely reliable laser ion source, functioning well for years.

The result that, for one range of parameters (3-ns neodymium glass laser pulses of 6-J energy on tantalum targets), the electron impact ionization (EII) (figure 20) was confirmed where the laser-produced plasma of very high density acts as in an ECR, but with very much higher ionization efficiency, can be used to conclude that one option could be to work with short wavelengths in order to increase further the ion density. Since appropriate excimer lasers with repetition of pulses reliably working for industry over very long periods are available now, this option at least may provide a comparably rather quick solution for the present problems with heavy ion sources for big accelerators.

Acknowledgments

The authors are grateful to several CERN staff members and visitors for stimulating discussions about this topic, especially Y. Amdidouche, C. Hill, A. Kuttenberger, K. Langbein, R. Matulieniene, J. Sellmair, B. Yu. Sharkov, T.R. Sherwood, A.V. Shumshurov, C.S. Taylor, and B. Williams. Thanks are also due to T. Henkelmann and G. Korschinek of the Technological University, Munich; to V.V. Apollonov of the Institute of General Physics, Academy of Sciences of Russia, Moscow; to V.B. Baranov and A.N. Starostin of the Troitsk Branch of the Kurchatov Institute in Moscow; and to Yu.A. Bykovski, Yu.P. Kosyrev, K.A. Monchinski, and Yu.Z. Oganesian at the Joint Institute for Nuclear Research, Dubna.

Our special thanks for support go to Prof. Dr. R. Höpfl of the Faculty of Electrical Engineering, Institute of Technology, Regensburg; to Dipl. Ing. Alois Schönberger; and for the most precise and reliable work—of such outstanding level that is rather rare today—to Dipl. Ing. Elke Anleitner.

REFERENCES

AHLSTROM, H.G. 1983 *Phys. Laser Fusion* (Nat. Tech. Inf. Service, Springfield, VA).

ALFVEN, H. 1988 *Laser Part. Beams* **6**, 385.

APOLLONOV, V.V. *et al.* 1970 *JETP Lett.* **11**, 252.

ARDENNE, M. VON 1956 *Atomkernenergie* **1**, 2015.

AMDIDOUCHE, Y. *et al.* 1992 *Rev. Sci. Instr.* **63**, 2838.

AYDIN, M. *et al.* 1992 *Laser Part. Beams* **10**, 155.

BARABASH, L.Z. *et al.* 1984 *Laser Part. Beams* **2**, 49.

BASOV, N.G. & KROKHIN, O.N. 1964 In *3rd Int. Quantum Electr. Conf. Paris 1963*, P. Grivet and N. Bloembergen, eds. (Dunod, Paris) Vol. 2, p. 1373.

BASOV, N.G. *et al.* 1986 *Heating and Compression of Thermonuclear Targets by Laser Beams* (Cambridge Univ. Press, Cambridge).

Downloaded from https://www.cambridge.org/core. University of Basel Library, on 11 Jul 2017 at 11:30:36, subject to the Cambridge Core terms of use, available at https://www.cambridge.org/core/terms. https://doi.org/10.1017/S0263034600010119

Basov, N.G. *et al.* 1987 *Sov. Phys. JETP* **65**, 727.

Becker, R. 1980 *Proc. ECR Workshop*, Darmstadt.

Begay, F. *et al.* 1983 *Observation of High Energy Heavy Ion Velocity Distribution in CO_2 Laser-Generated Plasmas*, 13th Anomalous Absorption Conference, Banff, June 1983, Los Alamos Nat. Lab., Report LA-UR-83-1603.

Biskamp, D. & Welter, H. 1975 *Plasma Physics and Controlled Fusion Research*, Tokyo, 1974 (IAEA, Vienna) Vol. 2, p. 507.

Bobin, J.L. 1985 *Phys. Rept.* **122**, 173.

Bohm, D. & Gross, E.P. 1949 *Phys. Rev.* **75**, 1851.

Boody, F. *et al.* 1996 *Laser and Part. Beams* **14**, 443.

Büchl, K. *et al.* 1972 In *Laser Interaction and Related Plasma Phenomena*, H. Schwarz and H. Hora, eds. (Plenum, New York) Vol. 2, p. 502.

Bykovski, Yu.A. *et al.* 1971 *Sov. Phys.-JETP* **33**, 706.

Chen, F.F. 1974 In *Laser Interaction and Related Plasma Phenomena*, H. Schwarz and H. Hora, eds. (Plenum, New York) Vol. 3A, p. 291.

Chen, H.H. & Liu, C.S. 1976 *Phys. Rev. Lett.* **37**, 693.

Chiao, R.Y. *et al.* 1964 *Phys. Rev. Lett.* **13**, 479.

Chirkov, B.V. 1990 *J. Phys.* **B23**, L103.

Cichitelli, L. *et al.* 1990 *Phys. Rev.* **A41**, 3121.

Clark, P.J. *et al.* 1985 In *AIP Proc. 130 Laser Acceleration of Particles*, C. Joshi and T. Katsuleas, eds. (Amer. Inst. Phys., New York), p. 380.

Collier, J. *et al.* 1996 *Laser and Part. Beams* **14**, 283.

Dawson, J.M. 1964 *Phys. Fluids* **7**, 981.

Deng, X. 1986 *Appl. Opt.* **25**, 377.

Denisov, N.G. 1957 *Sov. Phys. JETP* **4**, 544.

Drake, P.R. 1988 *Laser Part. Beams* **6**, 437.

Drake, P.R. *et al.* 1994 *Phys. Rev. Lett.* **13**, 2104.

Dragila, R. & Hora, H. 1982 *Phys. Fluids* **17**, 788.

Dubois, D.F. & Goldman, M.V. 1967 *Phys. Rev.* **164**, 201.

Dubois, D.F. 1974 *Laser Interaction and Related Plasma Phenomena*, H. Schwartz and H. Hora, eds. (Plenum, New York), Vol. 3A, p. 267.

Ehler, A.W. 1975 *J. Appl. Phys.* **46**, 2464.

Eidmann, K. & Sigel, R. 1974 *Laser Interaction and Related Plasma Phenomena*, H. Schwarz and H. Hora, eds. (Plenum, New York), Vol. 4B, p. 667.

Eliezer, S. & Hora, H. 1993 *Nuclear Fusion by Inertial Confinement*, G. Velarde, Y. Ronen, and J.M. Martinez-Val, eds. (IRC, New York), p. 42.

Eliezer, S. & Hora, H. 1989 *Phys. Rep.* **172**, 339.

Eliezer, S. & Hora, H. 1989a *Plasma Physics Varenna School of Inertial Confinement Fusion*, P. Caldriola, ed. (Soc. Fiz. Ital., Bologna), p. 375.

Engelhardt, A.G. *et al.* 1970 *Phys. Fluids* **13**, 212.

Fälthammar, C.G. 1988 *Laser Part. Beams* **8**, 437.

Försterling, K. 1950 *Archiv Elektr. Übertragungstech.* **5**, 209.

Gitomer, S.J. 1984, *20 Years of Plasma Research*, International Institute of Theoretical Physics, Trieste, September.

Gitomer, S.J. *et al.* 1986 *Phys. Fluids* **29**, 2679.

Giulietti, A. *et al.* 1989 *Laser Interaction with Plasmas*, G. Velarde *et al.*, eds. (World Scientific, Singapore), p. 208.

Goldsworthy, M.P. *et al.* 1986 *IEEE Trans. Plasma Sci.* **PS14**, 823.

Haseroth, H. & Hora, H. 1993 *Advances of Accelerator Physics and Technologies,* H. Schopper, ed. (World Scientific, Singapore), p. 465.

Häuser, T. *et al.* 1988 *J. Opt. Soc. Amer.* **B5**, 2029.

Häuser, T. *et al.* 1992 *Phys. Rev.* **A45**, 1278.

Downloaded from https://www.cambridge.org/core. University of Basel Library, on 11 Jul 2017 at 11:30:36, subject to the Cambridge Core terms of use, available at https://www.cambridge.org/core/terms. https://doi.org/10.1017/S0263034600010119

HENKELMANN, T. *et al.* 1991 *Nucl. Instr. Meth.* **B56/57**, 1152.
HENKELMANN, T. *et al.* 1992 *Rev. Sci. Instr.* **63**, 2828.
HERSHKOWITZ, N. 1985 *Space Sci. Rev.* **41**, 351.
HILL, C.E. & LANGBEIN, K. 1966 *Rev. Sc. Instr.* (Int. Conf. on Ion Sources, Vancouver 1995, in print).
HONIG, R.E. 1963 *Appl. Phys. Lett.* **3**, 8.
HÖPFL, R. *et al.* 1995 German Patent Appl. 195 13 566.0.
HORA, H. *et al.* 1957 *Zeitschr. f. Naturforsch. A* **22**, 278.
HORA, H. 1969 *Phys. Fluids* **12**, 182
HORA, H. 1969a *Zeitschr. f. Physik* **226**, 156.
HORA, H. 1971 *Laser Interaction and Related Plasma Phenomena*, H. Schwarz and H. Hora, eds. (Plenum, New York), Vol. 1, p. 273.
HORA, H. 1975 *J. Opt. Soc. Amer.* **65**, 882.
HORA, H. & KANE, E.L. 1977 *Appl. Phys.* **13**, 165.
HORA, H. *et al.* 1980 US-Pat. 4,199,685.
HORA, H. 1981 *Nuovo Cimento B* **64**, 1.
HORA, H. 1982 *Opt. Comm.* **41**, 268.
HORA, H. *et al.* 1984 *Phys. Rev. Lett.* **53**, 1650.
HORA, H. 1985 *Phys. Fluids* **28**, 3706.
HORA, H. & GHATAK, A.K. 1985a *Phys. Rev. A* **31**, 3473.
HORA, H. *et al.* 1989 *IEEE Trans. Plasma Sci.* **PS-17**, 284.
HORA, H. 1991 *Plasmas at High Temperature and Density* (Springer-Verlag, Heidelberg).
HORA, H. & AYDIN, M. 1992 *Phys. Rev. A* **45**, 6123.
HORA, H. 1996 *Nonlinear Force and Ponderomotion*, Inst. Laser E., Osaka Univ.
HORA, R.H. *et al.* 1992 *Laser Part. Beams* **10**, 175.
HUGHES, R.H. *et al.* 1980 *J. Appl. Phys.* **51**, 4088.
JOSHI, C. & CORKUM, P.B. 1995 *Physics Today* **48**(1), 36.
JONES, D.A. 1982 *Phys. Fluids* **25**, 2295.
KANE, E.L. & HORA, H. 1978 *Sov. J. Quant. Electron.* **8**, 7.
KORSCHINEK, G. & SELLMAIR, J. 1986 *Rev. Sci. Instr.* **57**, 745.
KORSCHINEK, G. & HENKELMANN, T. 1991 *Nucl. Instr. Meth. A* **302**, 376.
KATO, Y. *et al.* 1984 *Phys. Rev. Lett.* **53**, 1057.
KENTWELL, G.W. & HORA, H. 1970 *Plasma Phys.* **22**, 1051.
KEY, M. 1991 *Phys. World* **8**, 52.
KOROBKIN, V.V. & ALCOCK, A.J. 1968 *Phys. Rev. Lett.* **21**, 1433.
KRUER, W. 1986 *Physics of Laser Plasma Interaction* (Addison-Wesley, Reading, MA).
KUGLER, H. & HASEROTH, H. 1996 (private comm.).
KUTNER, V.B. *et al.* 1990 The Laser Ion Source of Multiply Charged Ions, Conference Seminar, Dubna.
LABAUNE, C. *et al.* 1985 *Phys. Rev. A* **22**, 577.
LÄDRACH, P. & BALMER, J.E. 1979 *Opt. Commun.* **31**, 350.
LALOUSIS, P. 1983 *Laser Part. Beams* **1**, 283.
LANDAU, L.D. 1946 *J. Phys. USSR* **10**, 25.
LANGBEIN, K. *et al.* 1990 *Rev. Sci. Instr.* **61**, 327.
LANGMUIR, I. 1929 *Phys. Rev.* **33**, 954.
LEHMBERG, R.H. & OBENSCHAIN, S.P. 1983 *Opt. Commun.* **46**, 27.
LEHMBERG, R.H. *et al.* 1987 *J. Appl. Phys.* **62**, 2680.
LICHTMAN, D. & READY, J.F. 1963 *Phys. Rev. Lett.* **10**, 342.
LINLOR, W.I. 1963 *Appl. Phys. Lett.* **3**, 210.
LIU, C.S. & ROSENBLUTH, M.N. 1974 *Phys. Fluids* **17**, 778.
LOTZ, W. 1967 *Zeitschr. Physik* **206**, 205.

Downloaded from https://www.cambridge.org/core. University of Basel Library, on 11 Jul 2017 at 11:30:36, subject to the Cambridge Core terms of use, available at https://www.cambridge.org/core/terms. https://doi.org/10.1017/S0263034600010119

Liu, C.S. & Rosenbluth, M.N. 1974 *Phys. Fluids* **17**, 778.

Lotz, W. 1967 *Zeitschr. Physik* **206**, 205.

Luther-Davies, B. & Roce, A.V. 1993 *Phys. Rev. A* **41**, 2154.

Maddever, R.A.M. *et al.* 1990 *Phys. Rev. A* **41**, 2154.

Maki, H. & Niu, K. 1987 *J. Phys. Soc. Japan* **45**, 269.

Marshak, R.E. 1941 *Ann. New York Acad. Sci.* **41**, 49.

Mayers, R.A., ed. 1986 *Encyclopedia of Physical Science and Technology*, 1st ed. (Academic Press, New York) Vol. 7, p. 99 (2nd ed. 1992, Vol. 8, p. 433).

McGuire, E. 1978 *Phys. Rev. A* **20**, 445.

Mochinski, K.A. 1991 private commun. Dubna, April.

Mroz, W. *et al.* 1994 *Rev. Sci. Instr.* **65**, 1272.

Nishihara, K. 1968 *J. Phys. Soc. Japan* **24**, 1152.

Nuckolls, J.H. 1982 *Phys. Today* **35**(9), 24.

Omari, T. *et al.* 1980 *Japan J. Appl. Phys.* **19**, L 728.

Oraevski, V.N. & Sagedeev, R.Z. 1963 *Sov. Phys. Tech. Phys.* **7**, 955.

Palmer, A.J. 1971 *Phys. Fluids* **114**, 2714.

Paul, W. 1990 *Rev. Mod. Phys.* **62**, 531.

Peacock, N.J. & Pease, R.S. 1969 *D* **2**, 1705.

Phipps, C. 1995 *Laser Part. Beams* **13**, 33.

Phipps, C.R. & Dreyfuss, R.W. 1993 *Laser Ionization Mass Analysis*, A. Vertes, R. Gijbels, and F. Adams, eds. (Chemical Analysis Series Vol. 124) (John Wiley, New York) p. 369.

Ready, J.F. 1965 *J. Appl. Phys.* **36**, 462.

Ready, J.F. 1971 *Effects of High Power Laser Radiation* (Academic Press, New York).

Richardson, R.C. & Alcock, A.J. 1971 *Appl. Phys. Lett.* **18**, 357.

Rode, A.V. 1983 Dissertation, Moscow Phys. Inst. Academ Sc., USSR.

Rowlands, T. 1990 *Plasma Phys. Control. Fusion* **32**, 279.

Schwarz, H.J. 1971 *Laser Interaction and Related Plasma Phenomena*, H. Schwarz and H. Hora, eds. (Plenum, New York), Vol. 1, p. 207.

Sharkov, B.Yu. *et al.* 1992 *Rev. Sci. Instr.* **63**, 2841.

Sharkov, B.Yu. *et al.* 1995 *Laser Interaction and Related Plasma Phenomena*, G.H. Miley and S. Nakai, eds. (AIP Conf. Proc.) (Am. Inst. Phys., New York).

Shearer, J.W. *et al.* 1970 *Bull. Amer. Phys. Soc.* **19**, 1483.

Shearer, J.W. & Eddleman, J.L. 1974 *Phys. Fluids* **16**, 1753.

Sherwood, T.R. 1995 *Laser Interaction and Related Plasma Phenomena*, G.H. Miley and S. Nakai, eds. (AIP Conf. Proc.) (Am. Inst. Phys., New York).

Sigel, R. *et al.* 1976 *Phys. Rev. Lett.* **36**, 1369.

Siegrist, M. *et al.* 1976 *Opt. Commun.* **18**, 609.

Silin, V.P. 1965 *Sov. Phys.-JETP* **21**, 1127.

Skupski, S. *et al.* 1989 *J. Appl. Phys.* **62**, 2680.

Spatschek, K.H. 1977 *Fortschr. Physik* **27**, 345.

Stamper, J.A. 1991 *Laser Part. Beams* **9**, 841.

Stenzel, R. 1976 *Phys. Fluids* **19**, 865.

Velarde, G. *et al.* 1993 *Nuclear Energy by Inertial Confinement* (Chem. Rubber Corp., Boca Raton, FL).

Wägli, P. & Donaldson, T.P. 1976 *Phys. Rev. Lett.* **40**, 457.

White, R.B. & Chen, F.F. 1974 *Plasma Phys.* **16**, 565.

Wong, A. & Stenzel, R. 1975 *Phys. Rev. Lett.* **34**, 727.

Woryna, E. *et al.* 1995 *Laser Interaction with Matter*, Oxford, 1994, S.J. Rose, ed. (Inst. Phys. Conf. Ser. No. 140) (Inst. of Phys., Bristol), p. 463.

Yonger, S.M. 1987 *Phys. Rev. A* **34**, 2841.

Zeitler, A. *et al.* 1985 *Phys. Fluids* **28**, 372.

Downloaded from https://www.cambridge.org/core. University of Basel Library, on 11 Jul 2017 at 11:30:36, subject to the Cambridge Core terms of use, available at https://www.cambridge.org/core/terms. https://doi.org/10.1017/S0263034600010119